Developmental Biology 492 (2022) 87–100

Contents lists available at ScienceDirect

Developmental Biology

journal homepage: www.elsevier.com/locate/developmentalbiology

Orthopedia expression during *Drosophila melanogaster* nervous system development and its regulation by microRNA-252

Kirsten Hildebrandt [a], Christine Klöppel [a], Jasmin Gogel [a], Volker Hartenstein [b], Uwe Walldorf [a,*]

[a] Developmental Biology, Saarland University, Building 61, 66421, Homburg, Saar, Germany
[b] Department of Molecular Cell and Developmental Biology, University of California, Los Angeles, CA, 90095, USA

ARTICLE INFO

Keywords:
Orthopedia (Otp)
Transcription factor
Drosophila brain
microRNA-252

ABSTRACT

During brain development of *Drosophila melanogaster* many transcription factors are involved in regulating neural fate and morphogenesis. In our study we show that the transcription factor Orthopedia (Otp), a member of the 57B homeobox gene cluster, plays an important role in this process. Otp is expressed in a stable pattern in defined lineages from mid-embryonic stages into the adult brain and therefore a very stable marker for these lineages. We determined the abundance of the two different *otp* transcripts in the brain and hindgut during development using qPCR. CRISPR/Cas9 generated *otp* mutants of the longer protein form significantly affect the expression of Otp in specific areas. We generated an *otp* enhancer trap strain by gene targeting and reintegration of Gal4, which mimics the complete expression of *otp* during development except the embryonic hindgut expression. Since in the embryo, the expression of Otp is posttranscriptionally regulated, we looked for putative miRNAs interacting with the *otp* 3′UTR, and identified microRNA-252 as a candidate. Further analyses with mutated and deleted forms of the microRNA-252 interacting sequence in the *otp* 3′UTR demonstrate an *in vivo* interaction of microRNA-252 with the *otp* 3′UTR. An effect of this interaction is seen in the adult brain, where Otp expression is partially abolished in a knockout strain of microRNA-252. Our results show that Otp is another important factor for brain development in *Drosophila melanogaster*.

1. Introduction

The *Drosophila orthopedia* (*otp*) gene codes for a homeodomain transcription factor (Simeone et al., 1994; Hildebrandt et al., 2020) and is a member of the 57B homeobox gene cluster together with *Drosophila Retinal homeobox* (*DRx*) (Eggert et al., 1998; Davis et al., 2003) and *homeobrain* (*hbn*) (Walldorf et al., 2000; Kolb et al., 2021). All three transcription factors are expressed in type I and type II neuroblasts in the brain and are important for progenitor cell proliferation leading to an expansion of the brain region compared with the ventral nerve cord (Curt et al., 2019). Otp is highly conserved among metazoa and orthologs have been studied in invertebrates such as the annelid *Platynereis dumerilii* (Tessmar-Raible et al., 2007), the mollusc *Patella vulgaris* (Nederbragt et al., 2002) and in sea urchins (Simeone et al., 1994). In vertebrates orthologs have been identified in zebrafish (Del Giacco et al., 2008), chicken (Simeone et al., 1994; Caqueret et al., 2005), mouse (Simeone et al., 1994) and human (Lin et al., 1999). In the *Drosophila* embryo Otp is expressed in the nervous system and the hindgut, and *otp* mutant alleles show a severe hindgut phenotype with a complete loss of the large intestine and a reduction of the anal pads (Hildebrandt et al., 2020). This hindgut phenotype, which is due to apoptosis in the developing hindgut, leads to embryonic lethality of *otp* mutant alleles (Hildebrandt et al., 2020).

Studies of *otp* in other systems, notably vertebrates, have mostly focused on the nervous system, where Otp is expressed in a conserved domain of the developing forebrain that gives rise to the alar hypothalamus. This domain gives rise to several populations of neurosecretory cells populating the paraventricular nucleus and supraoptic nucleus, as well as part of the amygdala (Simeone et al., 1994; Del Giacco et al., 2006; Bardet et al., 2008). Loss of *otp* results in the failure of these neurons to differentiate, with accompanying behavioral developmental and deficits caused by the absence of the corresponding neurohormones (Eaton et al., 2008; Filippi et al., 2012; Fernandes et al., 2013). The *otp*-positive alar hypothalamic domain shows other conserved genetic features, such as the exclusion of Sonic hedgehog (Shh) and Nkx2.1, a member of the vertebrate Nkx homeobox transcription factor family, and another neurodevelopmental determinant that (in the vertebrate forebrain) specifies the basal hypothalamic domain (Manoli and Driever,

* Corresponding author.
E-mail address: uwe.walldorf@uks.eu (U. Walldorf).

https://doi.org/10.1016/j.ydbio.2022.09.006
Received 15 July 2022; Received in revised form 5 September 2022; Accepted 19 September 2022
Available online 27 September 2022

2014). What has caught the attention of several researchers is the invariant, temporally maintained expression of *otp* from early to late stages, which is unusual for transcription factors which, generally, appear transiently at specific developmental times.

Among invertebrates, *otp* expression has been visualized in annelids (Tessmar-Raible et al., 2007) and planarians (Umesono et al., 1997, 1999). In the latter, *otp* appears in a lateral band of neurons populating the brain. In annelids, one finds a medial and lateral neuronal cluster of *otp*-positive cells. The medial cluster may well correspond to the *otp*-expressing neurosecretory domain described in vertebrates (Tessmar-Raible et al., 2007). Based on the expression of *otp* and other overlapping markers, including Nkx2.1 and Rx, these authors posit the existence of an evolutionarily conserved "apical brain", a neurosecretory center encountered in all bilaterian animals (Tessmar-Raible et al., 2007). The developmental fate of the lateral cluster of *otp*-expressing cells, observed in annelids as well as planarians, is not known. One of the goals of the present study was to elucidate how *otp* expression in *Drosophila* features in this framework of medial vs lateral domain. It has been reported that *otp* appears in the nervous system (Simeone et al., 1994; Hildebrandt et al., 2020), but details of its expression and role have remained unknown. In the present study we have analysed *otp* expression throughout development, and established a role in neural fate determination mediated by the miRNA-252.

Many developmental processes, including cell fate determination during nervous system development, are regulated by microRNAs (miRNAs). These miRNAs are 21–24 nucleotides long RNAs playing an important role in the posttranscriptional regulation of gene expression (Ambros, 2004). They are encoded in the genome, transcribed by RNA Polymerases II or III resulting in pri-miRNAs which are processed via Drosha and Dicer and bound by the RISC complex (see O'Brien et al., 2018 for review). The mature miRNA guides the RISC complex to a target mRNA which could be degraded or translationally inhibited depending on the homology between the miRNA and the target mRNA (Bagga et al., 2005; Lim et al., 2005; Wu and Belasco, 2008). In this way a single miRNA can influence the expression of up to 100 genes (Selbach et al., 2008). MiRNAs were first identified in the nematode *Caenorhabditis elegans* (Lee et al., 1993; Wightman et al., 1993), but also regulate a lot of processes in plants and higher organisms like mammals. Also in *Drosophila* miRNAs exist, here the miRNA *bantam* is well known as a regulator of wing development (Brennecke et al., 2003), regulator of the Hippo signaling (Thompson and Cohen, 2006) and the TGFβ pathway (Oh and Irvine, 2011). Another function of *bantam* is the regulation of the premature differentiation of neuroblasts (Weng and Cohen, 2015). MiRNA families will be grouped into classes depending on a 2 to 8 nucleotide long sequence at their 5′end, the so-called seed sequence, playing an important role during target recognition (Brennecke et al., 2005). Compared to higher organisms *Drosophila* has a smaller pool of miRNAs, nevertheless 80% of these have homologs in humans (Ibánez-Ventoso et al., 2008). For most *Drosophila* miRNAs transgenic fly strains exist that allow the expression of these individual miRNAs time and tissue dependent using the UAS/Gal4 system (Schertel et al., 2012; Bejarano et al., 2012).

In this paper we show that Otp is expressed in the brain in well-defined neuronal lineages that mostly fall outside the medial domain. To better characterize *otp* function there we used the CRISPR/Cas9 system and gene targeting to generate mutants affecting the otp-PE protein. The CRISPR/Cas9 induced *otp* mutants show a loss of Otp expression in defined areas of the larval brain. In addition we show *in vivo* that miRNA-252 is interacting with the 3′UTR of *otp* and thereby regulating its expression. In a miRNA-252 knockout strain we see a loss of Otp protein expression in a defined area of the adult brain. These findings reveal an important function of Otp during brain development of *Drosophila*.

2. Results

2.1. Otp expression pattern during development

Expression of *otp* in the nervous system starts at around embryonic stage 10, with small, segmentally reiterated clusters of neural precursor cells that form part of the ventral midline (mesectoderm) (Hildebrandt et al., 2020). At this stage, no labeling is detected in the brain. Brain expression of *otp* begins at stage 12 (germ band retraction) in neural precursors located in three domains designated as P1, P2 (protocerebrum) and D1 (deutocerebum; Fig. 1A, see also Hildebrandt et al., 2020). Using different optical sections we could now define the expression domains in more detail (Fig. 1B and C). Labeling of embryonic brains with an antibody against the neuronal marker Neurotactin (BP106) and other more specific markers (e.g., Fasciclin 3) reveals specific lineage-associated fiber bundles to which neuron clusters can be assigned (Hartenstein et al., 2015; Hartenstein, unpublished). The domain P1 corresponds to lineage cluster DPLI1-3 (Fig. 1B and C), domain P2 to lineage cluster DPLc1-4 (Fig. 1B) and domain D1 to lineage BAmv3 and, most likely, ventrally adjacent BAlc (Fig. 1B and C; for nomenclature see Wong et al., 2013; Ito et al., 2013; Yu et al., 2013; Hartenstein et al., 2015, Table 1). In a more ventral optical section expression in the lineage cluster BLAd is detected (Fig. 1C). Even more ventrally in the transition of the central brain to the suboesophageal ganglion neurons associated with the lineage tract of BAlp4 and other cells that likely correspond the lineage MD SA1 are Otp positive (Fig. 1D). An additional Otp expression domain is visible in the posterior dorsomedial region that gives rise to the DM lineages (Fig. 1A and B, white arrowheads).

To analyse the expression of Otp in the larval brain we used Neurotactin (Nrt) as a marker for secondary neurons (Barthalay et al., 1990) to highlight the brain in combination with Otp. The expression of Otp in a larval brain hemisphere is visible in several expression domains in the central brain region (Fig. 1E-L). Here it became obvious the Otp expression is detectable in lineages where Otp was already present in the embryo. Expression includes both primary neurons (born in the embryo) and secondary neurons (born in the larva) of the respective lineages. These include DPLl1-3 (Fig. 1F–I), DPLc2 and 4 (Fig. 1J–L), BLAd2, BAmv3 and BAlc (Fig. 1J-L), BAlp4 (Fig. 1I and J) and MD SA1 (Fig. 1K and L). In more posterior sections Otp expression was seen in the DM5 lineage (Fig. 1F), one of the six dorsomedial type II lineages. This would correspond to the embryonic expression of Otp in the dorsomedial region (Fig. 1A and B, white arrowhead). All these Otp expression domains are located in the central brain region whereas no expression was detectable in the optic lobe area.

The Otp expression in the adult brain was analysed in combination with Bruchpilot (Brp), a marker labeling synapses to mark the neuropile (Wagh et al., 2006). Again here the complete expression pattern of Otp in the adult brain is shown in Fig. 1M. Several expression domains are visible in the central brain region (Fig. 1M, white arrowheads), whereas the optic lobe shows no expression at all. The following detailed analysis to assign the expression to defined structures and lineages was done with help of the Virtual Fly Brain Atlas (Milyaev et al., 2012; Ito et al., 2014; Yu et al., 2013; Bates et al., 2020). Optical sections from anterior to posterior highlight the expression in the lineages BLAd (likely BLAd2, because this lineage expresses in the larva), BAmv3, BAlc and BAlp4 (Fig. 1N). In a section in the middle expression in DPLl3 is visible (Fig. 1O) and in the posterior section expression in DPLl1/2 and DPLc4 (likely DPLc4, because this lineage expresses in the larva; Fig. 1P). In this posterior brain region Otp is in addition to DM5 possibly also expressed in DM4 (Fig. 1P). In summary Otp expression in the adult is present in all lineages where it was already expressed in the embryonic and larval brain and therefore a very stable marker for these lineages.

2.2. Expression of different otp transcripts during development

For the *otp* gene nine different transcript forms are known falling into two different classes generating different protein forms (Flybase FB2022_03). We showed earlier that otp-RC, a representative of one class in the embryo is only expressed during hindgut development, whereas otp-RE, a representative of the other class is only expressed in the embryonic nervous system and brain (Fig. 2A) (Hildebrandt et al., 2020).

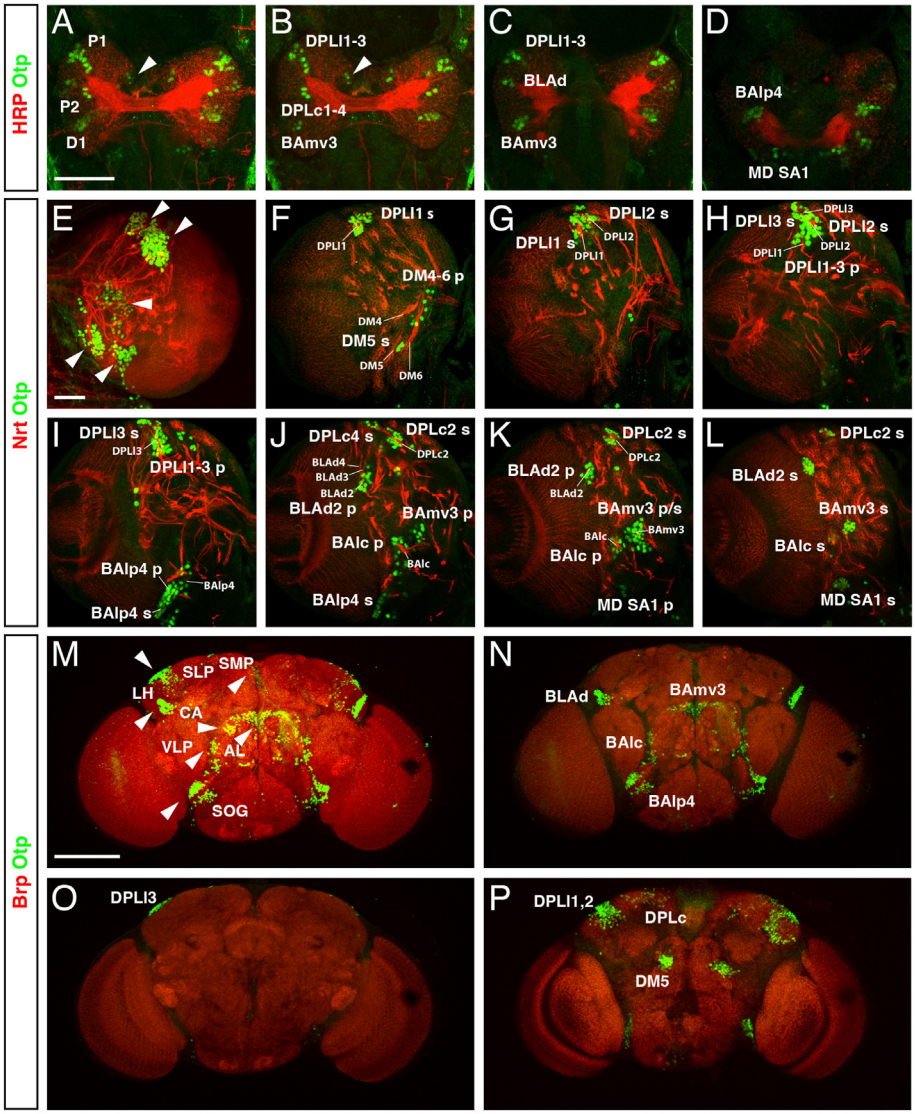

Fig. 1. Brain expression of Otp during development. Laser confocal images of *Drosophila* embryonic, larval and adult brains. (A-D) Expression of Otp in an embryonic brain at stage 16 using anti-Otp (green) and anti-HRP (red) stainings. (A) Complete expression pattern of Otp showing the already described expression domains P1, P2 and D1 (Hildebrandt et al., 2020) and an additional domain in the dorsomedial region (white arrowhead). (B-D) Three optical sections of the same embryonic brain from dorsal (B) to ventral (D) to show the identified Otp lineage expression. (E-L) Expression of Otp in a larval brain hemisphere using anti-Otp (green) and anti-Nrt (red) stainings. (E) Complete expression pattern showing the different Otp expression domains in the central brain region. (F-L) Seven optical sections of the larval brain hemisphere from dorsal (F) to ventral (L) showing the expression of Otp in identified. Otp-positive clusters are annotated in large letters, Nrt-positive tracts that define the lineage association of the clusters in small letters. The letter "p" following the lineage designation refers to primary neurons, "s" to secondary neurons. (M-P) Expression of Otp in the adult brain using anti-Otp (green) and anti-Brp (red) stainings. (M) Expression pattern of Otp showing the different expression domains in the adult brain (white arrowheads). (N–P) Three optical sections from anterior (N) to posterior (P) showing the adult expression domains. Lineage abbreviations: BAlc, basoanterior lineages, caudo-lateral subgroup; BAlp4, basoanterior lineages, posterolateral subgroup, 4; BAmv3, basoanterior lineages, ventromedial subgroup, 3; BLAd2, anterior basolateral lineages, dorsal subgroup, 2; DM5, dorsomedial lineage 5; DPLc1-4, lateral dorsoposterior lineages, central subgroup, 1–4; DPLl1-3, lateral dorsoposterior lineages, lateral subgroup, 1–3; MD SA1, mandibular suboesophageal anterior domain 1. Adult brain structure abbreviations: AL, Antennal Lobe; CA, Calyx; LH, Lateral Horn; SLP, Superior Lateral Protocerebrum; SMP, Superior Medial Protocerebrum; SOG, Suboesophageal Ganglion; VLP, Ventro Lateral Protocerebrum. (Scale bars: A-D, 50 μm; E-L, 50 μm; M-P, 25 μm).

Table 1
Lineage nomenclature.

Acronym Hartenstein et al. (2015)	Full name	Acronym Yu et al. (2013)
BAlc	Basoanterior laterocentral	ALl1
BAlp4	Basoanterior lateral posterior 4	ALlv1
BAmv3	Basoanterior medial ventral 3	ALad1
BLAd2	Basolateral anterior dorsal 2	SlPa1
DM4-6	Dorsomedial 4-6	DM4-6
DPLc4	Dorsoposterior lateral central 4	CLp1
DPLl1-3	Dorsoposterior lateral lateral 1-3	SLPp1, VLPd&p1, SLPad1

Since the hindgut expression of Otp stays on up to the adult stage (Hildebrandt et al., 2020) like the brain expression as shown here, one question arising was if the expression of both transcripts persists in this tissue specific manner during later stages. To address this question we performed qPCR experiments of larval and adult hindguts and brains. We designed specific primer pairs for the otp-RC and otp-RE transcripts that the PCR products are spanning exon-exon boundaries to ensure that cDNA and not genomic DNA is used preferentially as template in the qPCR experiments. For the qPCR experiments brains and hindguts from 50 larvae and adult flies were prepared, RNA isolated and cDNAs made by reverse transcription. The cDNAs were used for the qPCR experiments in technical triplicates using α-tubulin as a reference gene (Ponton et al., 2011). The qPCR experiments showed that in larvae, like in embryos, otp-RC is expressed only in the hindgut (Fig. 2B). The otp-RE transcript is expressed in the larval brain, but, in contrast to the embryo, also in the hindgut. Here, expression is 29 fold of that in the brain, and higher than otp-RC (Fig. 2B). A similar distribution of the two transcripts is detected at the adult stage. These qPCR experiments clearly show that the otp-RC transcript is hindgut specific during all developmental stages, whereas otp-RE is nervous system specific only in the embryo, but present in the brain and hindgut at later stages.

2.3. Generation of otp mutants by genome editing using the CRISPR/Cas9 system

Null mutants of *otp* are embryonic lethal due to its important function during embryonic hindgut development (Hildebrandt et al., 2020), an embryonic brain phenotype of *otp* mutants was not analysed yet. To investigate the function in the nervous system during later stages of development we used the CRISPR/Cas9 system to perform a genome editing affecting only otp-PE protein. In exon 2 which encodes the first 10

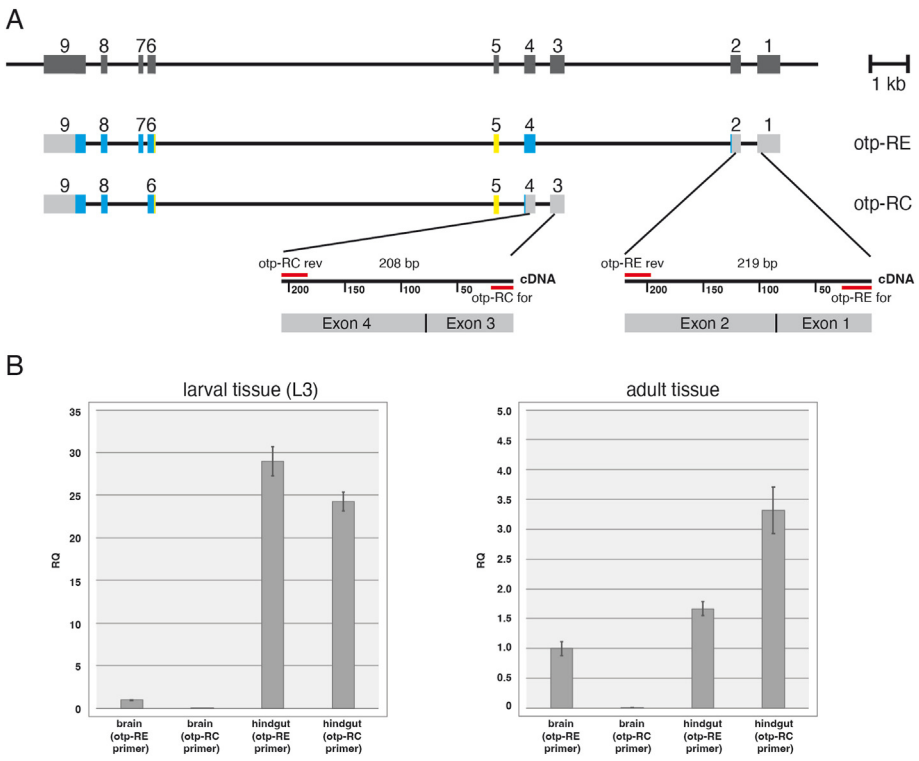

Fig. 2. Expression of the *otp* transcript variants otp-RC and otp-RE during development.
(A) Genomic organization of the *otp* gene with exons indicated as dark gray boxes. Below the two different transcripts otp-RE and otp-RC are shown (gray, untranslated region; blue, translated region; yellow, homeobox). The locations of the primers used for the qPCR experiments and the length of the PCR products are shown schematically below. (B) Relative quantification (RQ) of expression of otp-RE and otp-RC in wild-type L3 brains and hindguts (n = 50) by qPCR standardized to the otp-RE expression in the larval brain. (C) Relative quantification (RQ) of expression of otp-RE and otp-RC in wild-type adult brains and hindguts (n = 50) by qPCR standardized to the otp-RE expression in the adult brain.

amino acids of the otp-PE protein no suitable target site could be identified, therefore we used one in the exon 4 upstream of the ATG which is used in the otp-RC transcript. This would leave the otp-PC protein intact and introduce frame shift mutations resulting in a non-functional otp-PE protein. PCR analysis demonstrated that insertions and deletions, as well as a combination of both, were generated as expected (Fig. 3A). In some cases a few amino acids were deleted or added, leaving the reading frame intact (e.g., strains 33/1C, 32/1G and 33/3D; Fig. 3B), in other cases the open reading frame was altered leading to premature stop codons (e.g., strains 32/6A and 32/1F; Fig. 3B). These two strains would be the most favourable since they produce very short otp-PE proteins without a homeodomain which are most likely non-functional. All the isolated strains are not lethal and the animals survive up to the adult stage.

A comparison of the Otp expression in a wild type larval brain with larval brain of otp 32/6A animals showed a reduction of expression in the region of the DPLl1-3 lineages and in the region of the DM5 lineage (Fig. 3C and D, white arrowheads). In principle we expected a complete loss of Otp expression when the otp-PE protein isoform is affected. The presence of the remaining Otp expression might be due to a not yet identified splice variant of the *otp* gene, but the reduction of expression would argue, that some cells which normally express otp-PE are lost due to the mutation.

2.4. Generation of an otp mutant strain with reintegration of Gal4 in the otp locus

Since Otp turned out to be a very stable marker for a specific set of brain lineages, we generated an *otp* enhancer trap strain as a tool to visualize the expression pattern and to misexpress or downregulate genes in an *otp*-dependent pattern. We wanted to delete a part of the second exon of *otp* including the ATG used for the longer protein form otp-PE by gene targeting to generate a new *otp* allele affecting only this protein form which is exclusively expressed in the embryonic nervous system, but in later stages in addition to the nervous system also in the gut. Such an enhancer trap strain would ideally recapitulate the complete *otp* expression in the nervous system in heterozygous animals, whereas in homozygous animals the consequences of a loss of *otp* expression could be analysed. For the construction of such an *otp* gene targeting construct, we used the vector pTV^{cherry} (Baena-Lopez et al., 2013) that is suitable for this experimental design. We decided to delete a region of 64 bp starting 11 bp upstream of the ATG up to the first intron including the donor splice site (Fig. 4A, black arrowheads) and then reintegrated Gal4 to generate the strain otp^{KOGal4} (Fig. 4B).

To analyse this strain we visualized the Gal4 expression with the help of the mCD8:GFP marker and the H2B-mRFP1 marker. In the embryo expression of the nuclear RFP marker is colocalized in the brain in the three known cell clusters where Otp is expressed (Fig. 5A, yellow arrowheads) (Hildebrandt et al., 2020). In the ventral nerve cord Otp protein and the GFP marker are also colocalized up to the A2/A3 boundary (Fig. 5B, white arrowhead). Whereas Otp expression is not detected more posteriorly (Fig. 5B'), the GFP marker is present there (Fig. 5B''), arguing that the posttranscriptional regulation in that region is not working for the GFP marker. The prominent expression of Otp in the embryonic hindgut was not reproduced by either of the markers used (data not shown), therefore the hindgut module driving this expression (Kusch et al., 2002) is not capable of driving Gal4 expression in that tissue, maybe due to its location 3' of the integrated Gal4 gene. In the larval brain Otp and GFP marker expression are both seen in the brain hemispheres and the ventral ganglion and here again the specific expression boundary is visible (Fig. 5C, white arrowhead), but also here the GFP marker is expressed more posteriorly. In a higher magnification of the ventral ganglion this effect is better visible, here using the nuclear marker RFP (Fig. 5D). In larval brain hemispheres very nice colocalization of Otp and the markers GFP and RFP is detected (Fig. 5E and F, yellow arrowheads). The same is true for the coexpression in the adult brain (Fig. 5G). Next we also analysed the expression of the otp^{KOGal4} driven nuclear marker RFP in the larval alimentary tract. Here Otp is expressed in the larval hindgut, but not in the adjacent pylorus and in the rectum (Fig. 5H). In contrast the RFP marker is in addition to the hindgut also expressed in the rectum (Fig. 5I). In the adult alimentary tract, Otp is again expressed in the hindgut but here also in the rectum (Fig. 5J) and this expression is completely reproduced by the Gal4 induced RFP

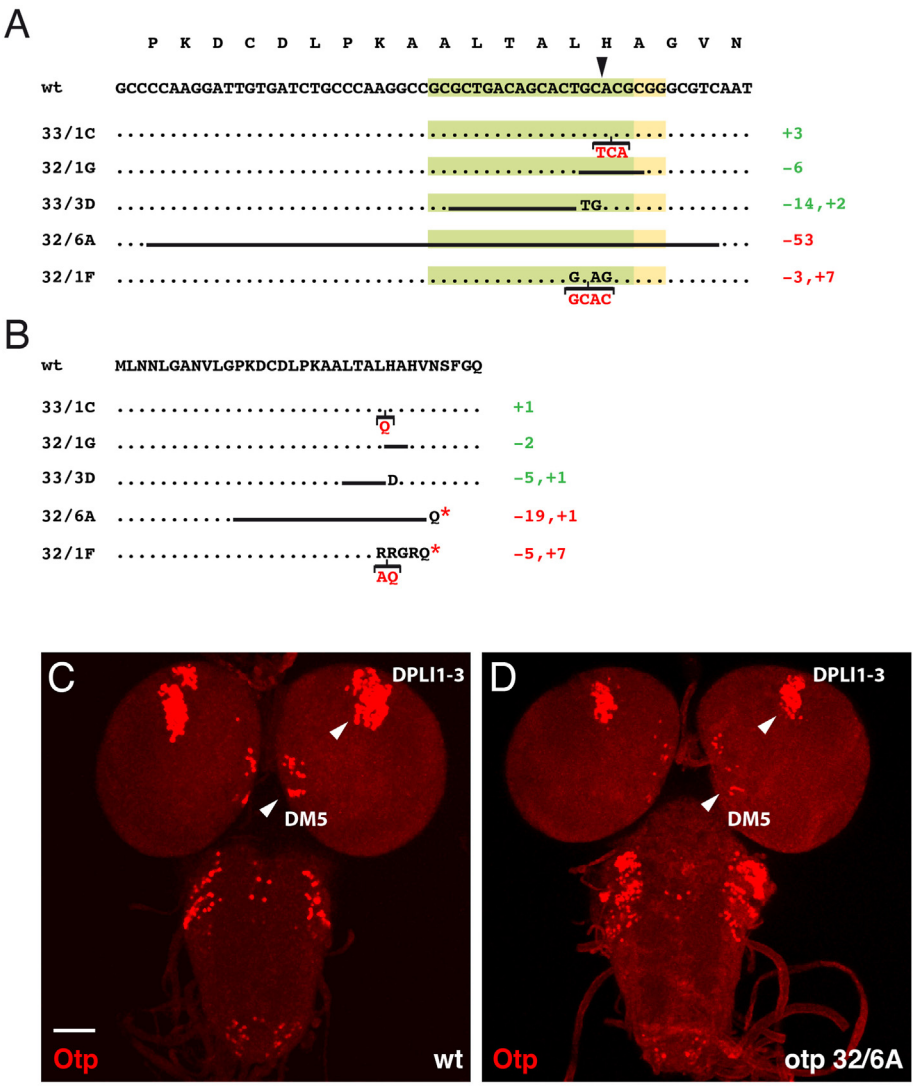

Fig. 3. CRISPR/Cas9 induced *otp* mutants.
(A) The *otp* wild-type sequence of the 5' part of exon 4 is indicated together with corresponding amino acids. The target sequence of the gRNA used is indicated in light green together with the neighbouring PAM (protospacer adjacent motif) sequence in light yellow. The Cas9 cleavage site is indicated by a black arrowhead. The DNA sequence alterations in five *otp* mutant strains are indicated below. Deletions are shown by black bars, insertions in red and changes of bases in black. For each strain changes in the reading frame are indicated, deletions and insertions not resulting in a frameshift in green, those resulting in a frame shift in red. (B) The wild-type amino acids are indicated together with alterations in the five *otp* mutant strains resulting from the CRISPR/Cas9 induced genome editing. Again amino acid insertions, alterations and deletions are indicated in red, black and as black bars. Changes not influencing the open reading frame are indicated in green, those changing the open reading frame in red. Stop codons are shown as red asterik. (C, D) Laser confocal images of *Drosophila* larval brains of wild-type (C) and otp 32/6A mutant animals (D). Expression of Otp is shown in red. A reduced Otp expression is seen in the DPLl1-3 region and the DM5 region of mutant animals (D, white arrowheads) compared to the wild type (C, white arrowheads). (Scale bar: 50 μm).

marker expression (Fig. 5K). In contrast to the embryo the larval expression in the gut might be regulated by a different regulatory element compared to the embryo, and there exists such a regulatory element upstream of the *otp* gene (data not shown). In summary the otp^{KOGal4} strain expression is recapitulating most expression patterns of Otp during development except the embryonic expression in the hindgut and might therefore considered as an otp-RE specific enhancer trap strain.

2.5. Interaction of miRNA-252 with otp

In previous work (Hildebrandt et al., 2020) we had noted that even though *otp* transcripts are expressed throughout the length of the embryonic VNC, the Otp protein is not expressed posterior to the A2/A3 boundary, indicating a posttranscriptional regulation of *otp*. MiRNAs are well known regulators of development that target specific mRNAs, leading to degradation of these mRNAs or a silencing of translation (O'Brien et al., 2018). To analyse a putative interaction of miRNAs with the *otp* mRNA we used a program predicting putative interaction sites in the 3′UTR of *otp* (www.microrna.org) and identified miRNA-100, miRNA-252, miRNA-316, miRNA-987 and miRNA-iab4-4-5p as putative interaction partners. To ascertain which of these miRNAs targets *otp* we generated an *otp* sensor-construct by fusing the *otp* 3′UTR to GFP and created transgenic flies which express the *otp* sensor-construct in all cells (Fig. S1). If in these flies a miRNA under UAS control is now activated in a specific domain using the UAS/Gal4 system, the miRNA will be ectopically expressed in that domain, resulting in the downregulation of the *otp* sensor. We used an *engrailed*-Gal4 strain (*en*-Gal4) to express the different UAS-miRNA strains in the posterior compartments of larval wing discs. The only UAS-miRNA strain which showed an effect in this assay was UAS-miRNA-252, here the GFP expression of the *otp* sensor was significantly reduced (Fig. S1). Therefore we only performed experiments with miRNA-252 to further confirm miRNA-252 as a regulator of *otp*. We made a construct consisting of enhanced GFP (eGFP) and the *otp* 3′UTR combined with a hsp70 minimal promotor and under control of 5xUAS binding sites (Fig. 6A) (Schertel et al., 2012). This construct could be co-expressed with a given UAS-miRNA at a location and time interval of choice. Through the coactivation in the same tissue, the effects of different UAS-miRNA strains can be compared and even quantified. In addition to the usage of a wild-type *otp* 3′UTR, we also used a UTR with a 23 bp deletion of the putative miRNA-252 seed sequence binding/interaction site and a 3 bp mutation in the seed sequence binding/interaction site which is absolutely required for the interaction of the miRNA with the 3′UTRs of target transcripts (Fig. 6B).

In a first set of experiments we used an *en*-Gal4 strain to express the different *otp* sensor-constructs in the posterior compartment of larval wing discs together with miRNA-252. We made the experiments in parallel to have the same conditions and here representative imaginal discs are shown (Fig. 7A–C). The expression of a wild-type *otp* 3′UTR construct results in a certain amount of GFP in the posterior compartment (Fig. 7A).

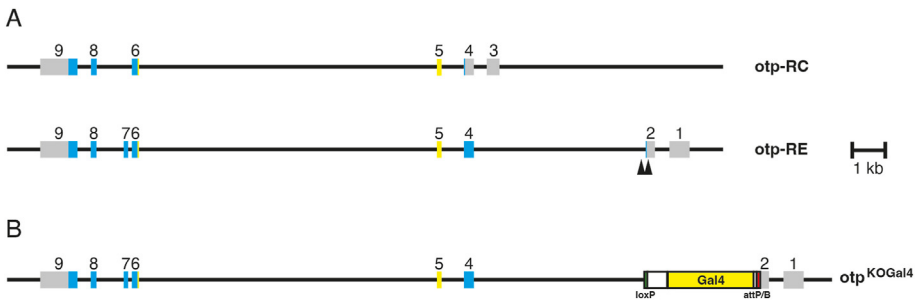

Fig. 4. Generation of the otp^{KOGal4} strain.
(A) The genomic organization of the *otp* locus with the exon regions leading to the two different transcripts otp-RC and otp-RE are shown. Noncoding regions are indicated by gray boxes, coding regions by blue boxes, the homeobox is shown in yellow. (B) The genomic organization of the otp^{KOGal4} strain is indicated. Here the region upstream of the ATG in exon 2 up to sequences shortly downstream of the exon 2 donor splice site is deleted (indicated by black arrowheads in (A)) and replaced by Gal4 (yellow) flanked by an attP/B site (red) and a loxP site (green).
Laser confocal images showing the expression of otp-^{KOGal4} heterozygous animals in different developmental stages visualized using an UAS-H2B-mRFP1 strain and an UAS-mCD8:GFP strain. (A) In a stage 16 embryo (the anterior end of the embryos is pointing down), Otp expression is shown in green and otp$^{KO-Gal4}$ dependent marker RFP expression in red. Coexpression of the nuclear marker RFP and Otp is seen in the embryonic brain in all three expression domains (yellow arrowheads). (B–B″) Staining of a ventral nerve cord of a stage 16 embryo, anterior is to the left. Otp staining is in red, GFP marker expression in green, single channels are shown in B′ and B″, the boundary with decreasing GFP expression is indicated by white arrowheads. (C) Dorsal view of a larval brain with Otp staining in red and GFP marker expression in green. The boundary of Otp expression in the ventral ganglion is indicated by a white arrowhead. (D) Otp staining (green) compared to the RFP marker expression (red) and Nrt (blue) in the ventral ganglion. Here the boundary of Otp expression is also shown by a white arrowhead, RFP marker expression is detected up to the posterior end. (E) Colocalization of Otp (red) and the marker GFP (green) in a larval brain hemisphere is detected (yellow arrowhead), Nrt is shown in blue. (F) Using the RFP marker (red) colocalization with Otp (green) is again seen in a larval brain hemisphere (yellow arrowhead), Nrt is again shown in blue. (G) In an adult brain colocalization of Otp (green) and the nuclear marker RFP (red) is seen in several regions. Adult brain structure abbreviations: AL, Antennal Lobe; CA, Calyx; LH, Lateral Horn; SLP, Superior Lateral Protocerebrum; SMP, Superior Medial Protocerebrum; SOG, Suboesophageal Ganglion; VLP, Ventro Lateral Protocerebrum. (H–K) Otp expression (green) and nuclear RFP expression (red) in larval (H, I) and adult (J, K) hindguts. Boundaries of specific structures are indicated by white arrowheads. Abbreviations: HG, hindgut; MG, midgut; PY, pylorus; RE, rectum.

When the seed sequence binding/interaction site in the 3′UTR is mutated, the miRNA interaction is decreased resulting in a higher eGFP expression (Fig. 7B). This effect is even more pronounced when the interacting sequences were deleted (Fig. 7C). To quantify this we used two different methods. First we analysed 20 images of wing discs for each *otp* construct to determine the relative fluorescence intensity using the software ImageJ (Fig. 7D), then we performed again qPCR experiments with mRNA isolated from 20 larvae of the different construct crosses to quantify the different eGFP mRNA levels. The constructs with the mutation and the deletion were standardized to the wild-type construct. As shown in Fig. 7D there is a slight increase of eGFP expression for the *otp* 3′UTR with the mutation or the deletion. This effect is more pronounced in the qPCR experiments, here the expression of the construct with the mutation of the seed sequence binding/interaction site is 3.6 times higher as the wildtype and the construct with the deletion 2.7 times higher (Fig. 7E). To repeat the experiments in another context we used a *deadpan* Gal4 strain (*dpn*-Gal4) to express GFP in the larval brain, here in the central brain mainly in neuroblasts in the type I lineages, in neuroblasts and INPs in the type II lineages and in the medulla region of the optic lobe. Like in the wing discs also in the brain a stronger eGFP expression was detected in constructs with the mutated (Fig. 7G) or deleted (Fig. 7H) seed sequence binding/interaction site. The quantification using microscopy showed again a similar effect of an increasing intensity (Fig. 7I) and the quantification using qPCR showed an increase of 1.3 times which is less compared to the previous experiments using *en*-Gal4, but still significant (Fig. 7J). These *in vivo* experiments clearly verify that miRNA-252 is indeed interacting with the *otp* 3′UTR in the predicted region.

2.6. *Effects of a miRNA-252 knockout on the otp expression*

To further characterize the regulatory interaction of miRNA-252 and *otp* we analysed *otp* expression in the targeted knockout strain miRNA-252 KO (Chen et al., 2014). MiRNA-252 is the most highly expressed

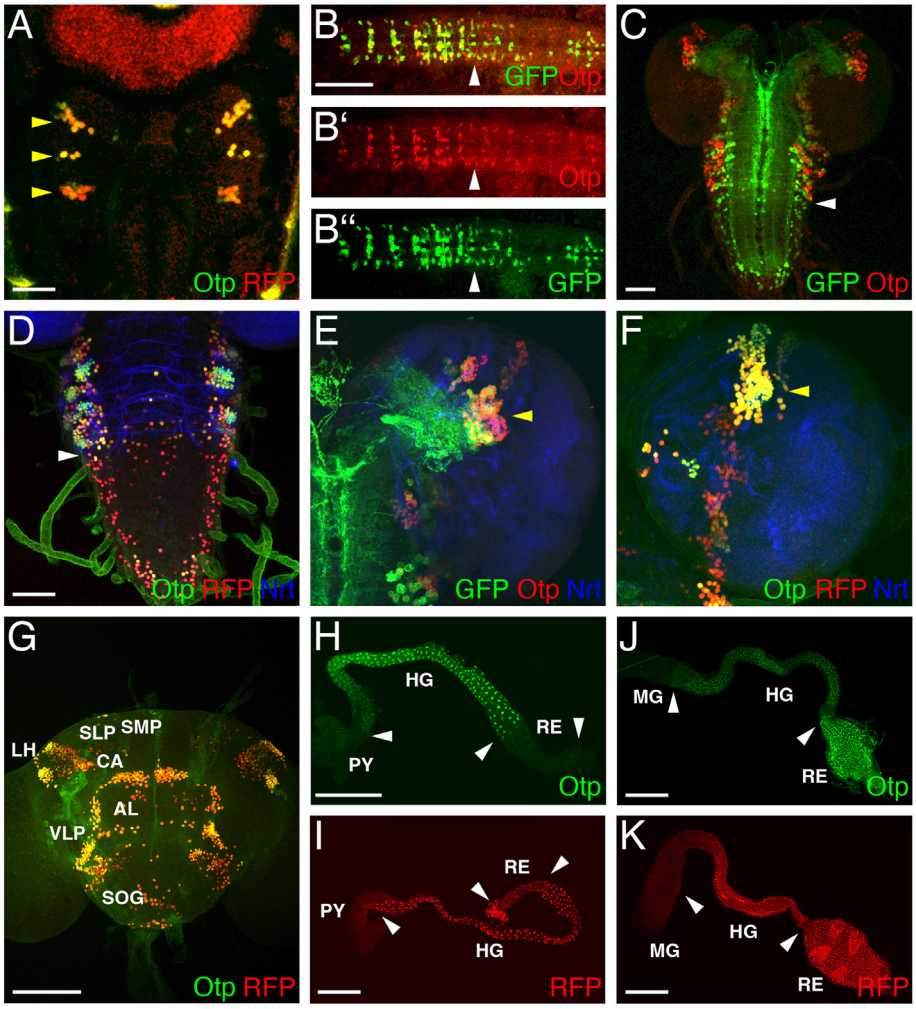

Fig. 5. Expression of the otp^{KOGal4} strain.

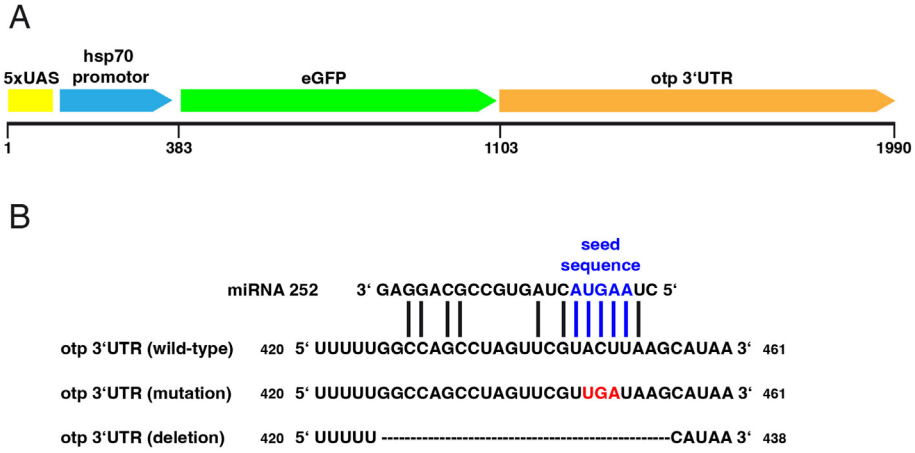

Fig. 6. *Otp* sensor-constructs.
(A) Schematic presentation of the UAS-*otp* sensor-construct consisting of 5xUAS binding sites (yellow), a hsp70 minimal promotor (blue), enhanced green fluorescent protein (eGFP) (green) and the *otp* 3'UTR (orange). (B) RNA sequences of the wild-type and modified *otp* 3′UTRs of the region where miRNA-252 interacts. Interaction of the miRNA-252 with *otp* 3′UTR is shown, the seed sequence is in blue. In the mutation construct changes in the seed sequence binding/interaction site are shown in red, the deleted area in the deletion construct is shown by an interrupted line.

miRNA in the adult fly head and involved in a large range of biological processes (Marrone et al., 2012). Embryonic brain expression of *otp* is unaltered in the miRNA-252 KO strain (Fig. 8A-C'). Also in the larval brain hemispheres (Fig. 8D, D') and the larval VNC (Fig. 8E, E') the expression pattern of Otp appears to be unaffected by the absence of the miRNA-252. Only in adult brains a subtle effect of miRNA-252 KO could be observed. Thus, whereas in the wild-type adult brain Otp expression is detected in a region dorsal of the Lateral Horn (LH) and the Superior Lateral Protocerebrum (SLP) (Fig. 8F, white arrowheads), most likely lineage DPLl3 (Milyaev et al., 2012), this expression pattern is missing in the adult brain of the miRNA-252 KO strain (Fig. 8F', white arrowheads). This effect might be in good agreement with the fact that miRNA-252 shows the highest expression in the adult brain and therefore might exert most of its function there.

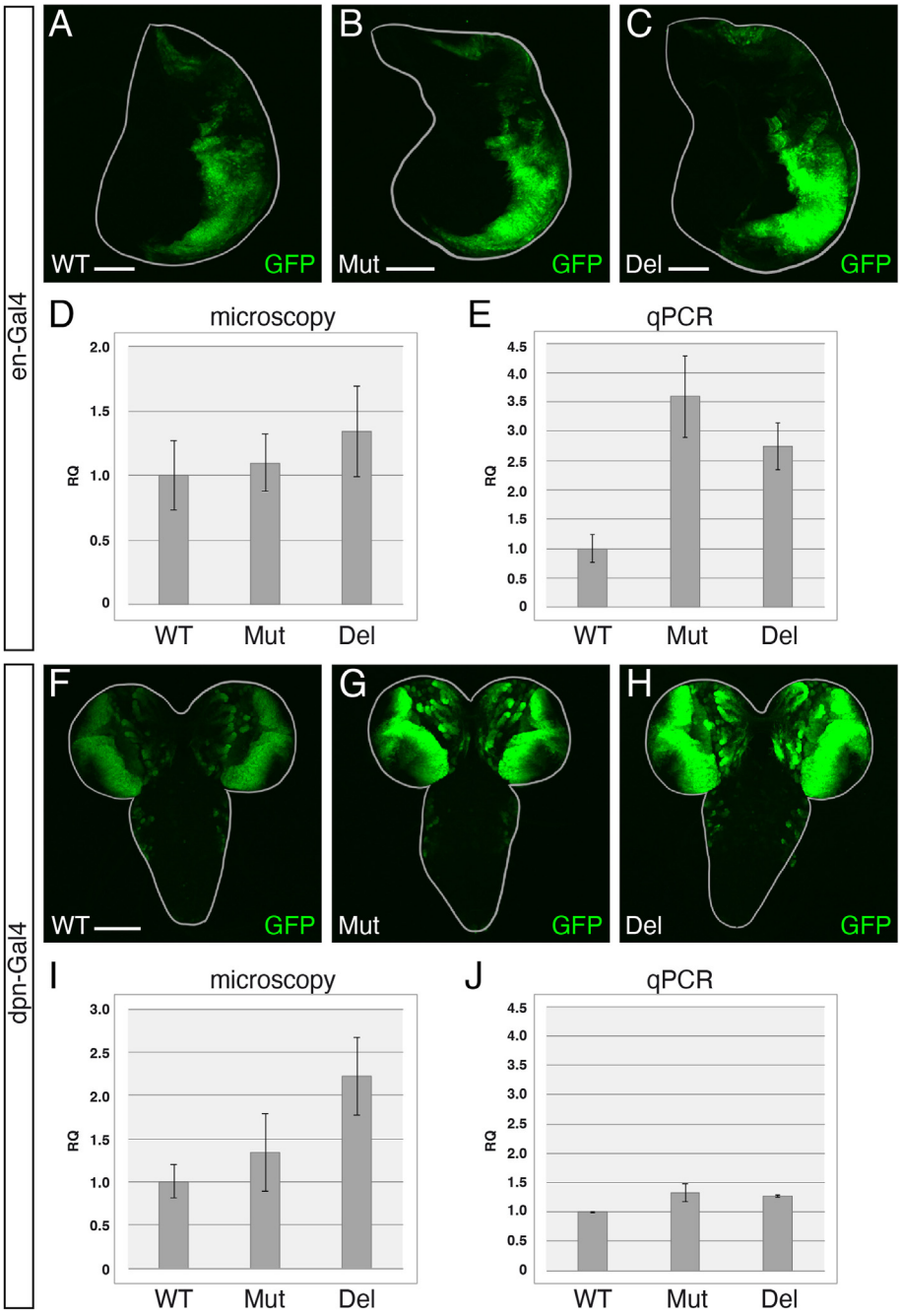

Fig. 7. *In vivo* analysis of the different Otp constructs. Confocal images of coexpression of the different UAS-*otp*-constructs (WT, wild-type; Mut, mutation; Del, deletion) together with a UAS-miRNA-252 strain using *en*-Gal4 to express both constructs in the posterior compartments (right site) of larval wing discs (A-C) and *dpn*-Gal4 for expression in the larval brain (F–H). Always representative discs and brains are shown (n = 20). Relative quantification (RQ) of fluorescence intensities of eGFP using microscopy images and ImageJ quantification are shown for the *en*-Gal4 experiments (D) and the *dpn*-Gal4 experiments (I). Relative quantification (RQ) of the different eGFP mRNA levels by qPCR are shown for the *en*-Gal4 experiments (E) and the *dpn*-Gal4 experiments (J).

3. Discussion

The *Drosophila orthopedia* gene was until now mainly analysed with respect to its expression and function during hindgut development (Hildebrandt et al., 2020). Here we analysed the expression and function of *otp* during nervous system development. Beginning at mid-embryonic stages, Otp is expressed in lineages of the protocerebrum (clusters DPLI, DPLc, BLAd, DM) and in the deutocerebrum (BAlc, BAlp4, BAmv3). Brain expression stays on during larval development up to the adult stage. Therefore Otp represents a very stable marker for these lineages.

Functionally, little is known about neurons of any of the protocerebral lineages DPLl, DPLc, or BLAd. DM lineages generate the columnar neurons of the central complex (Ito and Awasaki, 2008; Sullivan et al., 2019; Andrade et al., 2019), a center for navigation and spatial memory. Developmentally, these lineages are derived from the neurectodermal territory homologized with the dorsomedial domain (He et al., 2019; Farnworth et al., 2020). This domain, which gives rise to neuroendocrine cell populations, is also characterized by *otp* expression in other animals, including vertebrates and several invertebrate systems (e.g., the mollusc *Patella vulgaris* and the annelid *Platynereis dumerilii*; Tessmar-Raible et al., 2007). In *Drosophila*, the dorsomedial domain represents but a small portion of the *otp*-positive neural cell populations. Furthermore, even though we did not attempt double-labeling of Otp in conjunction with neuropeptide markers like DILP or corazonin, it is highly unlikely that any of the neurosecretory cells, which stand out by their large size and highly characteristic location, are Otp-positive.

Located outside (ventro-laterally of) the dorsomedial domain, the deutocerebral lineages BAlc, BAlp4 and BAmv3 give rise to interneurons of the *Drosophila* olfactory system (Das et al., 2013). The olfactory system has been studied intensively and is well characterized (Vosshall and

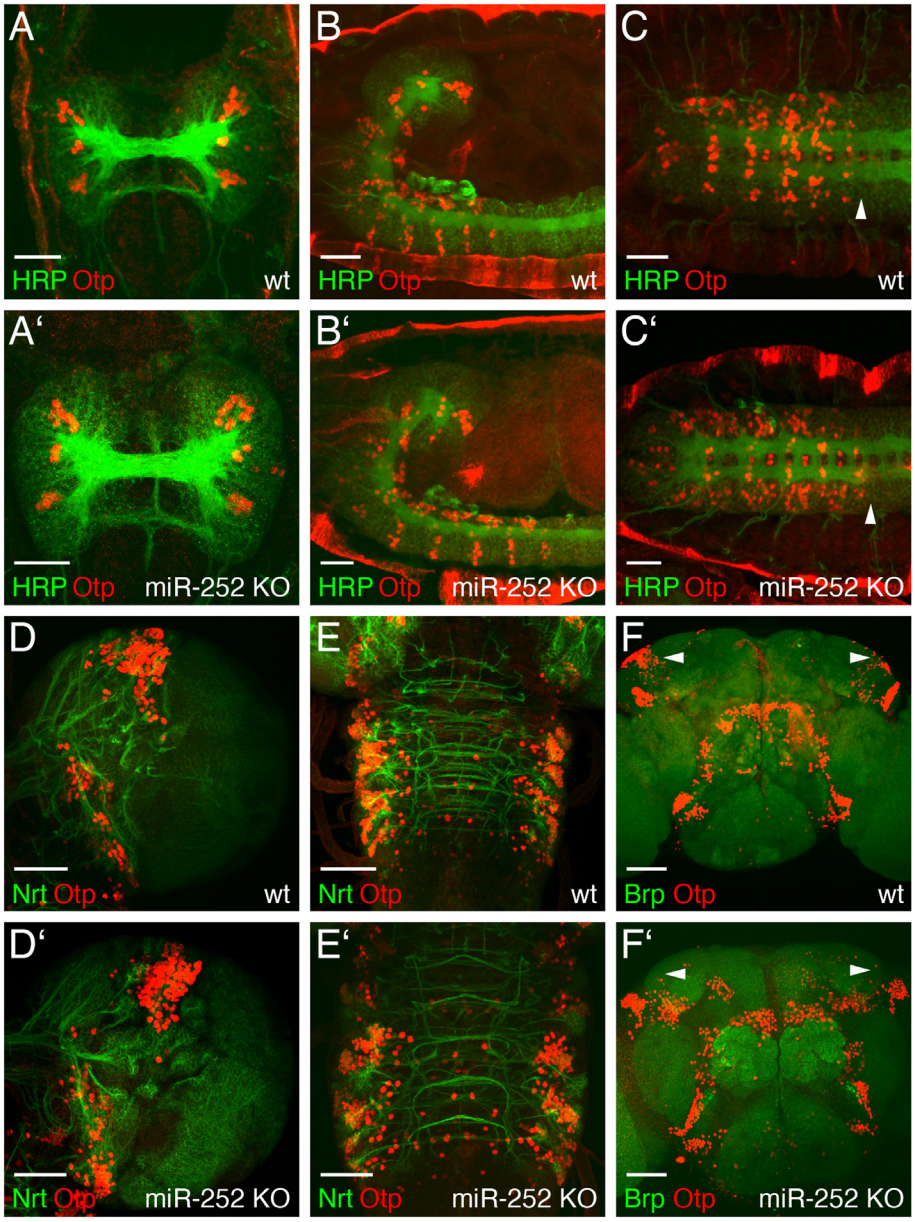

Fig. 8. Otp expression in wild-type and miR-252 knockout animals.
Laser confocal images of *Drosophila* embryonic, larval and adult brains of wild-type and miR-252 knockout animals. Expression of Otp is shown in red, HRP in embryos (A-C′), Nrt in larvae (D-E′) and Brp in adults (F, F′) is shown in green. Wild-type (wt) (A-F) or miR-252 knockout animals (miR-252 KO) (A′-F′) are indicated. (A, A′) Dorsal views of embryonic brains of stage 15 animals (the anterior end of the embryos is pointing down). (B, B′) Lateral views of stage 14 embryos showing the brain and anterior ventral nerve cord, anterior is to the left. (C, C′) Ventral views of the anterior part of ventral nerve cords, anterior is to the left. Otp expression is visible up to segment A3 (white arrowheads). (D, D′) Dorsal views of right larval brain hemispheres. (E, E′) Dorsal views of anterior parts of the ventral ganglia of larval brains. (F, F′) Anterior views of adult brains. The regions where Otp expression in the miR-252 KO strain is lost compared to the wild-type are indicated by white arrowheads.

Stocker, 2007). 1300 olfactory sensory neurons located on each antenna established connection to primary olfactory processing centers, the antennal lobes. There they make connections to 200 projection neurons and 100 local interneurons which project to higher brain centers in the lateral horn and mushroom body (Jefferis et al., 2001; Huang et al., 2010; Yaksi and Wilson, 2010). It will be important to analyse in more detail the role of *otp* in controlling the development and, possibly, function of olfactory interneurons.

In vertebrates Otp is expressed and required in the alar hypothalamus which gives rise to the supraoptic and paraventricular nuclei (SPV), as well as the medial amygdala. The SPV includes neuro-endocrine neurons involved in the regulation of the stress response, social behaviour and feeding behavior (Amir-Zilberstein et al., 2012; Gutierrez-Triana et al., 2014; Wircer et al., 2017; Moir et al., 2017). The medial amygdala is formed by interneurons that channel input from the olfactory bulb to the hypothalamus (Abellan et al., 2013; Biechl et al., 2017). It is therefore tempting to speculate about an evolutionary link between the expression pattern of *otp* in *Drosophila* and vertebrate brain. It is possible that *otp*, aside from its conserved role in specifying neuroendocrine cells (Tessmar-Raible et al., 2007), also acts as a determinant for neurons that form part of olfactory pathways that modulate fundamental behaviors like aggression, kin recognition or feeding.

It will be important to establish in how far signaling pathways and transcriptional regulators acting upstream of *otp* to specify its expression domain are conserved between vertebrates and *Drosophila*. Expression of *otp1* and *otp2* in zebrafish in the hypothalamic preoptic area (PO) (anterior alar plate) and the posterior tuberculum (PT) (posterior basal plate) is controlled by Nodal, Sonic hedgehog and Fibroblast Growth Factor 8 (Del Giacco et al., 2006). *Otp1* expression in hypothalamic neurons is also regulated by *prox1*, a vertebrate homolog of the *Drosophila* gene *prospero* (Dyer et al., 2003; Choski et al., 2006; Shimoda et al., 2006) and zinc-finger containing protein Fez1 (Levkowitz et al., 2003), a vertebrate homolog of the *Drosophila* gene *earmuff* (*erm*) (Weng et al., 2010). The same genes control *otp* expression in mouse, but here Sim1, a bHLH-PAS transcription factor (Michaud et al., 1998) acts in parallel to Otp without a cross regulation (Acampora et al., 1999; Wang and Lufkin, 2000). Additional factors that are co-expressed with Otp in the ventral forebrain and are switched on by the aforementioned signaling pathways

are the homeodomain transcription factors Six3/Six6 (Oliver et al., 1995; Jean et al., 1999; Ghanbari et al., 2001), Rx (Mathers et al., 1997; Deschet et al., 1999) and Nkx2.1/2 (Takuma et al., 1998), the Paired domain factor Pax6 (Kioussi et al., 1999) and the orphan nuclear receptor Tlx (Monaghan et al., 1995). In flies, genetic interactions between *otp* and any of these genes have not been studied so far. Based on similarity in expression, interactions between Otp and Erm, Nkx2.2 (*Drosophila* Vnd) and Shh (*Drosophila* Hh) are likely (V.H., unpublished). Other genes demarcating the dorsomedial domain, including homologs of Six3/Six6 (*Drosophila* Optix) and Rx are expressed earlier and in a much more restricted domain than the one giving rise to the *otp*-positive lineages, which suggests differences in the gene networks controlling *otp* expression in vertebrates and *Drosophila*.

Since *otp* mutants are embryonic lethal due to the very strong hindgut phenotype (Hildebrandt et al., 2020), later stages could only be analysed using clones. To avoid these restrictions, we generated an *otp* mutant which only affect the nervous system specific function through the mutation of the nervous system specific otp-PE isoform. Even this Otp protein isoform is also expressed in the hindgut in postembryonic stages, a loss of this isoform might not be so dramatic, since the otp-PC isoform is still present.

First, we used the CRISPR/Cas9 system to generate mutants which only affected the otp-PE proteins isoform. As expected, we could induce small deletions and/or mutations leading to changes of the open reading frame resulting in premature stop codons and shorter protein forms and we detected a reduced expression of *otp* in well-defined areas of the larval brain. The loss of the nervous system expression of *otp* might not result in dramatic changes of larger brain structures, but rather might have more subtle effects like influencing olfactory processes and/or learning and memory.

In addition to our CRISPR/Cas9 induced mutants we also generated an *otp* mutant affecting the otp-PE isoform by gene targeting deleting the ATG and adjacent sequences in exon 2. For this experiment we used the vector pTV^{cherry} (Baena-Lopez et al., 2013) which allows easier cloning of the homology arms used for the homologous recombination and a better selecting of the targeting flies. Our targeting efficiency of 1/775 was even better than those reported by Baena-Lopez et al. which were between 1/1000 and 1/2000. In similar experiments we made mutants using comparably small deletions for the genes *DRx* and *homeobrain* with efficiencies ranging between 1/600 and 1/700 (Klöppel et al., 2021; Hildebrandt et al., 2022), whereas for the *earmuff* gene a deletion of 1.5 kb resulted in a drop in the efficiency to 1/1894 (Hildebrandt et al., 2021). Using an attP site integrated in the *otp* locus instead of the deleted sequences it was then possible to reintegrate Gal4 into the locus to generate an *otp* Gal4 strain. This strain recapitulates the complete *otp* expression pattern during all stages of development and could even be used to analyse the expression in an otp-PE mutant background. Furthermore this Gal4 strain is an ideal tool to misexpress any gene in an *otp* dependent pattern using the UAS/Gal4 system (Brand and Perrimon, 1993) or to downregulate genes via RNAi with the RNAi strains available at VDRC (Dietzl et al., 2007) and Harvard University (Perkins et al., 2015).

miRNAs are known to regulate diverse genes and developmental processes through direct interactions within the 3′UTR of the respective genes. In our experiments we showed that miRNA-252 is directly interacting and thereby regulating *otp* expression. The *bantam* gene codes for the first miRNA identified in *Drosophila* (Brennecke et al., 2003). To analyse the regulation of the proapoptotic gene *hid* by *bantam*, a GFP sensor-construct was used where the *hid* 3′UTR with a *bantam* interaction sequence was fused to GFP and expressed in all cells of *Drosophila*. Wherever *bantam* was present, the GFP level was reduced and *bantam* activity could be shown in these experiments in the wing disc where it was known that bantam is expressed there (Brennecke et al., 2003). The drawback of these experiments was that one has to know where to look for the activity of the miRNA of interest. In later experiments the UAS/Gal4 system (Brand and Perrimon, 1993) was used for a specific activation of a certain UAS-miRNA construct in a well-defined tissue (Schertel et al., 2012) like we did it in our first experiments using *en*-Gal4 to express miRNA-252 in the posterior compartment of the *Drosophila* wing disc and thereby reducing the GFP expression there to show a direct interaction of miRNA-252 with the *otp* 3′UTR. We then used a more sophisticated version of this system which allows expressing both the sensor-construct and the miRNA simultaneously in any tissue of choice using again the UAS/Gal4 system. With this method we were able to show again the interaction of miRNA-252 with the 3′UTR of *otp* and even to quantify this by qPCR.

MiRNA-252 is an abundant miRNA and has 206 putative targets (Marrone et al., 2012). It is expressed in embryos and larvae, but stronger in pupal and adult stages (Lim et al., 2018). In the embryo an upregulation in neuroblasts, glia cells and neurons was described (Menzel et al., 2019). Such an upregulation is also seen in epithelial tumour tissue (Shu et al., 2017) and 60 h after an infection of flies with *Candida albicans* (Atilano et al., 2017). In addition ecdysone-responsive miRNA-252-5p controls the cell cycle by targeting Abi (Lim et al., 2018) and a developmental growth control during metamorphosis was shown through the direct targeting of *mushroom body tiny* (*mbt*) by miRNA-252 (Lim et al., 2019).

Our prediction would have been that a loss of miRNA-252 in flies using a miRNA-252 knockout strain (Chen et al., 2014) would lead to more Otp expression in certain tissues during development, maybe in the embryo where *otp* is posttranscriptionally regulated in the posterior segments of the nervous system. This was not the case, but we detected less Otp expression in a defined region of the adult brain in miRNA-252 knockout animals which are viable. But this would be the developmental stage when the miRNA-252 is most abundant in adult flies with a threefold enrichment in the head compared to the body (Marrone et al., 2012). There could be several reasons for this unexpected result. Most *C.elegans* miRNAs are not essential for development and function redundantly (Miska et al., 2007; Alvarez-Saavedra and Horvitz, 2010). Since this might also apply for *Drosophila* miRNAs, another miRNA might function redundantly to miRNA-252. The major effect of miRNA-252 on *otp* might be in a different tissue, maybe during gut development. Another possibility is that the loss of *otp* expression in the adult brain shows an indirect effect where miRNA-252 regulates a factor necessary for *otp* expression in that specific brain region. Future studies will be necessary to follow up this effect, but miRNA-252 is in general interesting to analyse, since is highly conserved in different organisms like *C.elegans*, *Drosophila* and humans (Ibánez-Ventoso et al., 2008; Ruby et al., 2007), and functions also in metamorphosis and growth regulation in hemimetabolan species like *Blatella germanica* (Rubio et al., 2012; Ylla et al., 2018).

Our data suppose an important function of *otp* during nervous system development which is also influenced by its regulation through miRNA-252. Using our CRISPR induced *otp* mutants and the *otp*-Gal4 enhancer trap strain, a much deeper analysis of the *otp* function in various processes of nervous system development might be possible in the future.

4. Methods

4.1. Fly strains

The following fly strains were used: yw^{67c23}; UAS-mCDC8:GFP, UAS-H2B-mRFP1 (Egger et al., 2010), ubiquitin-Gal4[3xP3-GFP] (Baena-Lopez et al., 2013), M {UAS-miRNA-252S} ZH-86Fb (Flyorf).

The following stocks were obtained from the Bloomington *Drosophila* Stock Center:

y[1] w[67c23]; sna[Sco]/CyO, P{w[+mC] = Crew}DH1 (BL 1092);

y[1] w[*]; Pin[Yt]/CyO; P{w[+mC] = UAS-mCD8:GFP.L}LL6 (BL 5130),

y[1] w[*]; P{w[+mW.hs] = en2.4-GAL4}e16 E P{w[+mC] = UAS-FLP.D}JD1 (BL 6356),

y[1] w[1118]; P{ry[+t7.2] = 70FLP}23 P{v[+t1.8] = 70I-SceI}4A/TM3, Sb[1] Ser[1] (BL 6935),

w[1118]; Df(2R)Exel7166/CyO (BL 7998),
y[1] w[1118]; PBac{y[+]-attP-3B}VK00033 (BL 9750),
y[1] M{RFP[3xP3.PB] GFP[E.3xP3] = vas-int.Dm}ZH-2A w[*]; PBac {y[+]-attP-3B}VK00033 (BL 24871),
y[1] w[*] P{y[+t7.7] = nos-phiC31\int.NLS}X; sna[Sco]/CyO (BL 34770),
w[1118]; P{y[+t7.7] w[+mC] = GMR13C02-GAL4}attP2 (BL 47859).
y[1] M{w[+mC] = nos-Cas9.P}ZH-2A w[*] (BL 54591),
y[1] w[67c23]; Sco/CyO
w[1118]; TM3/TM6B.

4.2. qPCR experiments

For the qPCR experiments RNA was isolated from 20 total larvae, 50 larval and adult brains or 50 larval and adult hindguts using the ISOLATE II RNA Micro Kits (Bioline) for tissues and the ISOLATE II RNA Mini Kit (Bioline) for total larvae. CDNA was synthesized from 200 ng RNA from the tissues or 1000 ng RNA from total larvae using the QuantiTect Reverse Transcription Kit (Qiagen). The qPCR experiments were performed using the QuantiTect SYBR® Green PCR Kit (Qiagen) according to the supplier. Experiments were done as technical triplicates. The following primer pairs were used: otp-RC for (5′-GCTCTTTTGCGGCGCAC-3′) and otp-RC rev (5′-GCCGGAGGATCCACCACC-3′); otp-RE for (5′-GAACTCTGACCCCAGCC-CATAAC-3′) and otp-RE rev (5′-GGGAATCGATATCGACTGGTGG-3′); ForGFP (5′-GCAACTACAAGACCCGC-3′); RevGFP (5′-GTCGGCCATGA-TATAGACG-3′). For control experiments the primers ForTubulin (5′-TGTCGCGTGTGAAACACTTC-3′) and RevTubulin (5′-AGCAGGCGTTTC-CAATCTG-3′) (Ponton et al., 2011) were used. The evaluation of the qPCR results was done according to the ΔΔCt method.

4.3. gRNA design, cloning of CRISPR otp construct and analysis of CRISPR/Cas9 induced mutations

A suitable target site in exon 4 of *otp* was selected to mediate Cas9 induced cleavage in exon 4. To avoid off-target cleavage, target sites were selected using the CRISPR target finder (http://tools.flycrispr.molbio.wisc.edu/targetFinder/) (Gratz et al., 2013). Target site primers were annealed and cloned in the vector pCFD3-dU6:3 (Port et al., 2014) cut with BbsI according to www.crisperflydesign.org. The primers used were: CRISPR-Otp2A (5‘-GTCGCGCGCTGACAGCACTGCACG-3‘) and CRISPR-Otp2B (5‘-AAACCGTGCAGTGCTGTCAGCGCG-3‘). Correct constructs were identified by PCR and PCR products sequenced by Starseq (Mainz, Germany). Transgenic fly lines were generated by PhiC31-integrase mediated transformation (Bischof et al., 2007) in the attP2 site (68A4) using strain BL 25710 and standard techniques (Rubin and Spradling, 1982). Transformants with the individual CRISPR constructs were crossed to a *nanos*-Cas9 strain (BL 54591) and individual males of the offspring balanced over CyO. The Cas9 target region from individual strains was PCR amplified using primers 5‘ and 3‘ of the target region (primers sequences are available upon request) and sequencing of the PCR products was performed by Starseq (Mainz, Germany).

4.4. Generation of an otp gene targeting construct and reintegration of Gal4

An *otp* donor gene targeting construct was made in the vector pTV^{cherry} according to Baena-Lopez et al. (2013). The two 2.5 kb homology arms were amplified using Q5 High-Fidelity DNA Polymerase (New England Biolabs) and BACR10P11 DNA (Hoskins et al., 2000). The primers otpGT1A (5’-GCGGCCGCAACAACGAATTGAGATGTTATCACG-3′) and otpGT2A (5′-GGTACCAATTGCGGATCGACAGAGTCGAC-3′) were used for homology arm 1 and otpGT3A (5′-ACTAGTATAGCGTTTTAAGTGCGGGCTGC-3′) and otpGT4A (5′-GGCGCGCCAGATCAAGATGACGCAGTAGTCTC-3′) for homology arm 2. All primers came with unique restriction enzyme recognition sites added to their end (underlined), which enabled later cloning in the final vector. After adding 3′ adenine overhangs to the two PCR products they were subcloned into the vector pCR-XL-TOPO (ThermoFisher Scientific, Waltham, Massachusetts, USA) and some clones sequenced by Starseq (Mainz, Germany). From correct clones the homology arms were cutted out with the relevant restriction enzymes and finally cloned in the vector pTV^{cherry} (Baena-Lopez et al., 2013). P-element-mediated transformation of some constructs into w^{1118} flies was performed by Bestgene (Chino Hills, California, USA). Transformants were balanced, and transformants with a non-lethal integration on the third chromosome were used for the generation of final targeting strain to avoid negative effects if some P-element sequences still remain at that position after recombination of the vector cassette in the *otp* locus. Transformants were crossed with *hs-Flp, hs-SceI* flies (BL 6935) and resulting larvae were heat-shocked at 48 h and 72 h after egg laying for 1 h at 37 °C. Two hundred adult female flies with mottled red eyes were crossed with *ubiquitin-Gal4[3xP3-GFP]* males and the progeny screened for the presence of red-eyed flies. The transgene *ubiquitin-Gal4[3xP3-GFP]* was removed by selection against GFP expression and the resulting targeting flies were balanced over CyO and molecularly analysed for the correct integration event. Among 27130 flies in the offspring of our gene targeting crosses we identified 35 red-eyed flies resulting in a targeting frequency of 1/775. Some of these flies were balanced and analysed by PCR to verify that the homologous recombination was correct. For the PCR reactions we used primers within the cassette introduced by the recombination events and primers located outside of the homology arms. Primers otpGT5A (5‘-TTTTGCTGCCGATAACGCCTTTG-3‘) and mCherryrev2 (5‘-CCTCGTCGTCGTTCAGGTTG-3‘) were used for the upstream region and pTVGal4-1 (5‘-CGTTTTTATTGTCAGGGAGT-GAGTTTGC-3 and otpGT6A (5‘-GCAGCCCTAACTGTTCATCGTG-3‘) for the downstream region. From one of these strains, called otp^{KO}, removal of the *white* gene was performed by crossing of the *otp*-targeting flies to a strain expressing Cre Rekombinase (BL 1092) and selecting for and balancing of white eyed flies among the cross offspring. For the reintegration of Gal4 in the *otp* locus the vector RIV^{Gal4} was used (Baena-Lopez et al., 2013). First, *otp* targeting flies were crossed with PhiC31-expressing flies (BL 34770) and embryos of that cross injected with RIV^{Gal4} DNA. Red-eyed transformant flies were selected and the *white* marker was again removed using the loxP sites to generate the strain otp^{KOGal4}.

4.5. Generation of the different otp sensor-constructs

For the wild-type *otp* 3’UTR we used the primers otpmiR3 (5‘-TATACTCGAGAATTTGTTGAAAAGCTTCGAAAGCTTT-3’) and otpmiR4 (5‘-TATACTCGAGAGTTGGATTTAAATTTAGGCTTAAACG-3’) and amplified a 0.9 kb fragment by PCR. This fragment was cloned into the vector pCR2.1 TOPO (ThermoFisher Scientific, Waltham, Massachusetts, USA) and some clones sequenced by Starseq (Mainz, Germany). From a correct clone the fragment was cut out using the XhoI sites generated via the otpmiR3 and otpmiR4 primers (underlined sequences) and cloned into the vector pUAST-eGFPattB (Schertel et al., 2012). To make different versions of the *otp* 3′UTR we used the Splicing by Overlap Extension PCR (SOE PCR) (Horton et al., 1993). We used the primers Del seed miRNA252 3′UTR-otpA (5‘-CAATAATTTTTCATAATTACGCCTAATTGTTTAGGAATGT-3‘) and Del seed miRNA252 3’UTR-otpB (5‘-CGGCCGTAATTATGAAAAATTATTG-TAACGCCACGTGGATAC-3‘) for the deletion and Mut seed miRNA252 3’UTR-otpA (5‘-CAATAATTTTTGGCCAGCCTAGTTCGTTGATAAGCA-TAATTACGC-3‘) and Mut seed miRNA252 3’UTR-otpB (5‘-CTAAA-CAATTAGGCGTAATTATGCTTATCAACGAACTAGGCTGGC-3‘) for the mutation within the *otp* 3'UTR in combination with the otpmiR3 and otpmiR4 primers. The corresponding PCR products were then also cloned via the pCR2.1 TOPO vector into the vector pUAST-eGFPattB. From the three different *otp* sensor-constructs transgenic flies with insertions on the third chromosome were generated using the strain BL 24871. We then recombined the different *otp* sensor-constructs integrated in the third chromosome with the UAS-miRNA-252 construct which is also integrated in the third chromosome. Through the appropriate crosses flies were generated that carry the appropriate Gal4 construct, the UAS miRNA-252 construct

and the respective *otp* sensor-constructs.

4.6. Immunocytochemistry

Embryos were collected, dechorionated with 50% bleach for 2 min, washed with 0.1% NaCl/0.1% Triton X-100 and fixed for 12 min in 3.7% formaldehyde in PEM (100 mM PIPES, 1 mM EGTA, 1 mM $MgCl_2$) and heptane. After removal of both phases, embryos were devitelinized in equal volumes of heptane and methanol by 2 min of vigorous shaking and washed three times with methanol. The 3rd instar larvae and adult tissues were dissected in 1x phosphate buffered saline (PBS), fixed for 60 min in 2% paraformaldehyde in PBL and washed three times with 1x PBS containing 0.2% Triton X-100 (PBX) and then incubated for 3 × 5 min in methanol. Fixed embryos or larval tissues were washed 3 × 5 min and 6 × 30 min in PBX and blocked for 30 min in 5% normal horse serum and 10% PBX in PBS. Incubations with primary antibodies were performed overnight at 4 °C. Samples were washed 3 × 5 min and 6 × 30 min in PBX and blocked for 30 min in 5% normal horse serum and 10% PBX in PBS. After an overnight incubation with secondary antibodies at 4 °C embryos or larval tissues were washed 3 × 5 min and 6 × 30 min in PBX and mounted in Vectashield (Vector Laboratories). Adult tissues were treated the same as larval tissues but were incubated with the appropriate antibody two nights each. Primary antibodies were guinea-pig anti-Otp antibody (1:1000), goat FITC-conjugated anti-Hrp antibody (1:100) (ICN Biomedical/Cappel); mouse anti-Brp (nc82) (1:25) and mouse anti-Nrt (BP106) antibody (1:25) were obtained from the Developmental Studies Hybridoma Bank, Iowa. Secondary antibodies were Alexa Fluor 488, 568 and 647 goat anti-mouse IgG (H + L) antibodies and Alexa Fluor 488 and 568 goat anti-guinea-pig IgG (H + L) antibodies (ThermoFisher Scientific, Waltham, Massachusetts, USA), all used at a 1:1000 dilution. Stained embryos were mounted in Vectashield H-1000 (Vector Laboratories, Burlingame, Canada).

4.7. Microscopy

For fluorescence microscopy a Leica TCS SP5 confocal microscope (Leica, Wetzlar, Germany) with a HyD detector and a constant laser speed of 8000 Hz or a variable detector using 400 Hz with a 40× objective was used. Optical sections from 0.5 μm up to 1 μm intervals were acquired and combined to show the relevant structure or expression domain completely. Captured images from optical sections were arranged and processed using FIJI and ImageJ (NIH. Md., USA) and Adobe Photoshop and Illustrator (Adobe Systems, San Jose, CA, USA).

(Scale bars: A-C, 25 μm; D-G, 50 μm; I, 25 μm; H, J, K, 10 μm).
(Scale bars: A-C, 25 μm; F-G, 25 μm like in F).
(Scale bars: A-C′, 25 μm; D-F′, 50 μm).
(Scale bar: 50 μm).

Ethical approval and consent to participate

Not applicable; no vertebrate or human subjects.

Consent for publication

All authors have approved this manuscript.

Declarations of competing interest

None.

Data availability

Data will be made available on request.

Acknowledgements

Stocks obtained from the Bloomington *Drosophila* Stock Center (NIH P40OD018537) were used in this study. We are grateful to Boris Egger, Luis Alberto Baena-Lopez, Jean-Paul Vincent and Ya-Wen Chen for fly stocks and vectors, the Developmental Studies Hybridoma Bank for antibodies, the BACPAC Resources Center (BPRC) for BAC clones. We thank Doris Jann and Susanne Speicher-Mentges for technical assistance and Peter Lipp for using the confocal microscope. We thank the anonymous reviewers for their comments and suggestions which improved the manuscript.

Appendix A. Supplementary data

Supplementary data to this article can be found online at https://doi.org/10.1016/j.ydbio.2022.09.006.

References

Abellan, A., Desfilis, E., Medina, L., 2013. The olfactory amygdala in amniotes: an evo-devo approach. Anat. Rec. 296, 1317–1332.
Acampora, D., Postiglione, M.P., Avantaggiato, V., Di Bonito, M., Vaccarino, F.M., Michaud, J., Simeone, A., 1999. Progressive impairment of developing neuroendocrine cell lineages in the hypothalamus of mice lacking the *Orthopedia* gene. Genes Dev. 13, 2787–2800.
Alvarez-Saavedra, E., Horvitz, H.R., 2010. Many families of *C. elegans* microRNAs are not essential for development or viability. Curr. Biol. 20, 367–373.
Ambros, V., 2004. The functions of animal microRNAs. Nature 431, 350–355.
Amir-Zilberstein, L., Blechmann, J., Sztainberg, Y., Norton, W.H.J., Reuveny, A., Borodovsky, N., Tahor, M., Bonkowsky, J.L., Bally-Cuif, L., Chen, A., Levkowitz, G., 2012. Homeodomain protein Otp and activity-dependent splicing modulate neuronal adaptation to stress. Neuron 73, 279–291.
Andrade, I.V., Riebli, N., Nguyen, B.M., Omoto, J.J., Cardona, A., Hartenstein, V., 2019. Developmentally arrested precursors of pontine neurons establish an embryonic blueprint of the *Drosophila* central complex. Curr. Biol. 29, 412–425.
Atilano, M.L., Glittenberg, M., Monteiro, A., Copley, R.R., Ligoxygakis, P., 2017. MicroRNAs that contribute to coordinating the immune response in *Drosophila melanogaster*. Genetics 207, 163–178.
Baena-Lopez, L.A., Alexandre, C., Mitchell, A., Pasakarnis, L., Vincent, J.-P., 2013. Accelerated homologous recombination and subsequent genome modification in Drosophila. Development 140, 4818–4825.
Bagga, S., Bracht, J., Hunter, S., Massirer, K., Holtz, J., Eachus, R., Pasquinelli, A.E., 2005. Regulation by let-7 and lin-4 miRNAs results in target mRNA degradation. Cell 122, 553–563.
Bardet, S.M., Martinez-de-la-Torre, M., Northcutt, R.G., Rubenstein, J.R.L., Puelles, L., 2008. Conserved pattern of OTP-positive cells in the paraventricular nucleus and other hypothalamic sites of tetrapods. Brain Res. Bull. 75, 231–235.
Barthalay, Y., Hipeau-Jacquotte, R., de la Escalera, S., Jiménez, F., Piovant, M., 1990. *Drosophila* neurotactin mediates heterophilic cell adhesion. EMBO J. 9, 3603–3609.
Bates, A.S., Schlegel, P., Roberts, R.J.V., Drummond, N., Tamimi, I.F.M., Turnbull, R., Zhao, X., Marin, E.C., Popovici, P.D., Dhawan, S., et al., 2020. Complete connectomic reconstruction of olfactory projection neurons in the fly brain. Curr. Biol. 16, 3183–3199.
Bejarano, F., Bortolamiol-Becet, D., Dai, Q., Sun, K., Saj, A., Chou, Y.T., Raleigh, D.R., Kim, K., Ni, J.Q., Duan, H., et al., 2012. A genome-wide transgenic resource for conditional expression of *Drosophila* microRNAs. Development 139, 2821–2831.
Biechl, D., Tietje, K., Ryu, S., Grothe, B., Gerlach, G., Wullimann, M.F., 2017. Identification of accessory olfactory system and medial amygdala in the zebrafish. Sci. Rep. 14, 44295.
Bischof, J., Maeda, R.K., Hediger, M., Karch, F., Basler, K., 2007. An optimized transgenesis system for *Drosophila* using germ-line-specific phiC31 integrases. Proc. Natl. Acad. Sci. U. S. A 104, 3312–3317.
Brand, A.H., Perrimon, N., 1993. Targeted gene expression as a means of altering cell fates and generating dominant phenotypes. Development 118, 401–415.
Brennecke, J., Hipfner, D.R., Stark, A., Russell, R.B., Cohen, S.M., 2003. *Bantam* encodes a developmentally regulated microRNA that controls cell proliferation and regulates the proapoptotic gene *hid* in *Drosophila*. Cell 113, 25–36.
Brennecke, J., Stark, A., Russell, R.B., Cohen, S.M., 2005. Principles of microRNA-target recognition. PLoS Biol. 3, e85.
Caqueret, A., Coumailleau, P., Michaud, J.L., 2005. Regionalization of the anterior hypothalamus in the chick embryo. Dev. Dynam. 233, 652–658.
Chen, Y.W., Song, S., Weng, R., Verma, P., Kugler, J.M., Buescher, M., Rouam, S., Cohen, S.M., 2014. Systematic study of *Drosophila* microRNA functions using a collection of targeted knockout mutations. Dev. Cell 31, 784–800.
Choski, S.P., Southall, T.D., Bossing, T., Edoff, K., de Wit, E., Fischer, B.E., van Steensel, B., Micklem, B., Brand, A.H., 2006. Prospero acts as a binary switch between self- renewal and differentiation in *Drosophila* neural stem cells. Dev. Cell 11, 775–789.
Curt, J.R., Salmani, B.Y., Thor, S., 2019. Anterior CNS expansion driven by brain transcription factors. Elife 8, 45274.

Das, A., Gupta, T., Davla, S., Prieto-Godino, L.L., Diegelmann, S., Reddy, O.V., Raghavan, K.V., Reichert, H., Lovick, J., Hartenstein, V., 2013. Neuroblast lineage-specific origin of the neurons of the *Drosophila* larval olfactory system. Dev. Biol. 373, 322–337.

Davis, J., Tavsanli, B.C., Dittrich, C., Walldorf, U., Mardon, G., 2003. *Drosophila retinal homeobox* (*drx*) is not required for establishment of the visual system, but is required for brain and clypeus development. Dev. Biol. 259, 272–287.

Del Giacco, L., Sordino, P., Pistocchi, A., Andreakis, N., Tarallo, R., Di Benedetto, B., Cotelli, F., 2006. Differential regulation of the zebrafish *orthopedia I* gene during fate determination of diencephalic neurons. BMC Dev. Biol. 6, 50.

Del Giacco, L., Pistocchi, A., Cotelli, F., Fortunato, A.E., Sordino, P., 2008. A peek inside the neurosecretory brain through *Orthopedia* lenses. Dev. Dynam. 237, 2295–2303.

Deschet, K., Bourrat, F., Ristoratore, F., Chourrout, D., Joly, J.S., 1999. Expression of the medaka (*Oryzias latipes*) Ol-RX3 paired-like gene in two diencephalic derivates, the eye and the hypothalamus. Mech. Dev. 83, 179–182.

Dietzl, G., Chen, D., Schnorrer, F., Su, K.C., Barinova, Y., Fellnerm, M., Gasser, B., Kinsey, K., Oppel, S., Schleibauer, S., et al., 2007. A genome-wide transgenic RNAi library for conditional gene inactivation in *Drosophila*. Nature 448, 151–156.

Dyer, M.A., Livesey, F.J., Cepko, C.L., Oliver, G., 2003. Prox1 function controls progenitor cell proliferation and horizontal cell genesis in the mammalian retina. Nat. Genet. 34, 53–88.

Eaton, J.L., Holmqvist, B., Glasgow, E., 2008. Ontogeny of vasotocin-expressing cells in zebrafish: selective requirement for the transcriptional regulators *orthopedia* and *single-minded 1* in the preoptic area. Dev. Dynam. 237, 995–1005.

Egger, B., Gold, K.S., Brand, A.H., 2010. Notch regulates the switch from symmetric to asymmetric neural stem cell division in the *Drosophila* optic lobe. Development 137, 2981–2987.

Eggert, T., Hauck, B., Hildebrandt, N., Gehring, W.J., Walldorf, U., 1998. Isolation of a *Drosophila* homolog of the vertebrate homeobox gene *Rx* and its possible role in brain and eye development. Proc. Natl. Acad. Sci. U. S. A 95, 2343–2348.

Farnworth, M.S., Eckermann, K.N., Bucher, G., 2020. Sequence heterochrony led to a gain of functionality in an immature stage of the central complex: a fly-beetle insight. PLoS Biol. 18, e3000881.

Fernandes, A.M., Beddows, E., Filippi, A., Driever, W., 2013. Orthopedia transcription factor *otpa* and *otpb* paralogous genes function during dopaminergic and neuroendocrine cell specification in larval zebrafish. PLoS One 8, e75002.

Filippi, A., Jainok, C., Driever, W., 2012. Analysis of transcriptional codes for zebrafish dopaminergic neurons reveals essential functions of Arx and Isl1 in prethalamic dopaminergic neuron development. Dev. Biol. 369, 133–149.

Ghanbari, H., Seo, H.C., Fjose, A., Brändli, A.W., 2001. Molecular cloning and embryonic expression of *Xenopus* Six homeobox genes. Mech. Dev. 101, 271-217.

Gratz, S.J., Cummings, A.M., Nguyen, J.N., Hamm, D.C., Donohue, L.K., Harrison, M.M., Wildonger, J., O'Connor-Giles, K.M., 2013. Genome engineering of *Drosophila* with the CRISPR RNA-guided Cas9 nuclease. Genetics 194, 1029–1035.

Gutierrez-Triana, J.A., Herget, U., Lichtner, P., Castillo-Ramirez, L.A., Ryu, S., 2014. A vertebrate-conserved *cis*-regulatory module for targeted expression in the main hypothalamic regulatory region for the stress response. BMC Dev. Biol. 14, 41.

Hartenstein, V., Younossi-Hartenstein, A., Lovick, J.K., Kong, A., Omoto, J.J., Ngo, K.T., Viktorin, G., 2015. Lineage-associated tracts defining the anatomy of the *Drosophila* first instar larval brain. Dev. Biol. 406, 14–39.

He, B., Buescher, M., Farnworth, M.S., Strobl, F., Stelzer, E.H., Koniszewski, N.D., Muehlen, D., Bucher, G., 2019. An ancestral apical brain region contributes to the central complex under the control of foxQ2 in the beetle *Tribolium*. Elife 8, e49065.

Hildebrandt, K., Bach, N., Kolb, D., Walldorf, U., 2020. The homeodomain transcription factor Orthopedia is involved in development of the *Drosophila* hindgut. Hereditas 157, 46.

Hildebrandt, K., Kübel, S., Minet, M., Fürst, N., Klöppel, C., Steinmetz, E., Walldorf, U., 2021. Enhancer analysis of the *Drosophila* zinc finger transcription factor Earmuff by gene targeting. Hereditas 158, 41.

Hildebrandt, K., Kolb, D., Klöppel, C., Kaspar, P., Wittling, F., Hartwig, O., Federspiel, J., Findji, I., Walldorf, U., 2022. Regulatory modules mediating the complex neural expression patterns of the *homeobrain* gene during *Drosophila* brain development. Hereditas 159, 2.

Horton, R.M., Ho, S.N., Pullen, J.K., Hunt, H.D., Cai, Z., Pease, L.R., 1993. Gene splicing by overlap extension. Methods Enzymol. 217, 270–279.

Hoskins, R.A., Nelson, C.R., Berman, B.P., Laverty, T.R., George, R.A., Ciesiolka, L., Naeemuddin, M., Arenson, A.D., Durbin, J., David, R.G., et al., 2000. A BAC-based physical map of the major autosomes of *Drosophila melanogaster*. Science 287, 2271–2274.

Huang, J., Zhang, W., Qiao, W., Hu, A., Wang, Z., 2010. Functional connectivity and selective odor responses of excitatory local interneurons in *Drosophila* antennal lobe. Neuron 67, 1021–1033.

Ibánez-Ventoso, C., Vora, M., Driscoll, M., 2008. Sequence relationships among *C.elegans, D.melanogaster* and human microRNAs highlight the extensive conservation of microRNAs in biology. PLoS One 3, e2818.

Ito, K., Awasaki, T., 2008. Clonal unit architecture of the adult fly brain. Adv. Exp. Med. Biol. 628, 137–158.

Ito, M., Masuda, N., Shinomiya, K., Endo, K., Ito, K., 2013. Systematic analysis of neural projections reveals clonal composition of the *Drosophila* brain. Curr. Biol. 23, 644–655.

Ito, K., Shinomiya, K., Ito, M., Armstrong, J.D., Boyan, G., Hartenstein, V., Harzsch, S., Heisenberg, M., Homberg, U., Jenett, A., et al., 2014. A systematic nomenclature for the insect brain. Neuron 81, 755–765.

Jean, D., Bernier, G., Gruss, P., 1999. Six6 (Optx2) is a novel murine Six3-related homeobox gene that demarcates the presumptive pituitary/hypothalamic axis and the ventral optic stalk. Mech. Dev. 84, 31–40.

Jefferis, G.S., Marin, E.C., Stocker, R.F., Luo, L., 2001. Target neuron prespecification in the olfactory map of *Drosophila*. Nature 414, 204–208.

Kioussi, C., O'Connell, S., St-Onge, L., Treier, M., Gleiberman, A.S., Gruss, P., Rosenfeld, M.G., 1999. Pax6 is essential for stablishing ventral-dorsal cell boundaries in pituitary gland development. Proc. Natl. Acad. Sci. U. S. A 96, 14378–14382.

Klöppel, C., Hildebrandt, K., Kolb, D., Fürst, N., Bley, I., Karlowatz, R.J., Walldorf, U., 2021. Functional analysis of enhancer elements regulating the expression of the *Drosophila* homeodomain transcription factor DRx by gene targeting. Hereditas 158, 42.

Kolb, D., Kaspar, P., Klöppel, C., Walldorf, U., 2021. The *Drosophila* homeodomain transcription factor Homeobrain is involved in the formation of the embryonic protocerebrum and the supraesophageal brain commissure. Cell. Dev. 165, 203657.

Kusch, T., Storck, T., Walldorf, U., Reuter, R., 2002. Brachyury proteins regulate target genes through modular binding sites in a cooperative fashion. Genes Dev. 16, 518–529.

Lee, R.C., Feinbaum, R.L., Ambros, V., 1993. The *C.elegans* heterochronic gene lin-4 encodes small RNAs with antisense complementarity to lin-14. Cell 75, 843–854.

Levkowitz, G., Zeller, J., Sirotkin, H.I., French, D., Schilbach, S., Hashimoto, H., Hibi, M., Talbot, W.S., Rosenthal, A., 2003. Zinc finger protein too few controls the development of monoaminergic neurons. Nat. Neurosci. 6, 28–33.

Lim, D.H., Lee, S., Han, J.Y., Choi, M.S., Hong, J.S., Seong, Y., Kwon, Y.S., Lee, Y.S., 2018. Ecdysone-responsive microRNA-252-5p controls the cell cycle by targeting Abi in *Drosophila*. Faseb. J. 32, 4519–4533.

Lim, D.H., Lee, S., Han, J.Y., Choi, M.S., Hong, J.S., Lee, Y.S., 2019. MicroRNA miR-252 targets *mtb* to control the developmental growth of *Drosophila*. Insect Mol. Biol. 28, 444–454.

Lim, L.P., Lau, N.C., Garrett-Engele, P., Grimson, A., Schelter, J.M., Castle, J., Bartel, D.P., Linsley, P.S., Johnson, J.M., 2005. Microarray analysis shows that some microRNAs downregulate large numbers of target mRNAs. Nature 433, 769–773.

Lin, X., State, M.W., Vaccarino, F.M., Greally, J., Hass, M., Lackman, J.F., 1999. Identification, chromosomal assignment, and expression analysis of the human homeodomain-containing gene *Orthopedia* (*OTP*). Genomics 60, 96–104.

Manoli, M., Driever, W., 2014. *nkx2.1* and *nkx2.4* genes function partially redundant during development of the zebrafish hypothalamus, preoptic region, and pallium. Front. Neuroanat. 8, 145.

Marrone, A.K., Edeleva, E.V., Kucherenko, M.M., Hsiao, N.H., Shcherbata, H.R., 2012. Dg-Dys-Syn1 signaling in *Drosophila* regulates the microRNA profile. BMC Cell Biol. 13, 26.

Mathers, P.H., Grinberg, A., Mahon, K.A., Jamrich, M., 1997. The *Rx* homeobox gene is essential for vertebrate eye development. Nature 387, 603–607.

Menzel, P., McCorkindale, A.L., Stefanow, S.R., Zinzen, R.P., Meyer, I.M., 2019. Transcriptional dynamics of microRNAs and their targets during *Drosophila* neurogenesis. RNA Biol. 16, 69–81.

Michaud, J.L., Rosenquist, T., May, N.R., Fan, C.M., 1998. Development of neuroendocrine lineages requires the bHLH-PAS transcription factor SIM1. Genes Dev. 12, 3264–3275.

Milyaev, N., Osumi-Sutherland, D., Reeve, S., Burton, N., Baldock, R.A., Armstrong, J.D., 2012. The virtual fly brain browser and query interphase. Bioinformatics 28, 411–415.

Miska, E.A., Alvarez-Saavedra, E., Abbott, A.L., Lau, N.C., Hellman, A.B., McGonagle, S.M., Bartel, D.P., Ambros, V.R., Horvitz, H.R., 2007. Most Caenorhabditis elegans microRNAs are individually not essential for development or viability. PLoS Genet. 3, e215.

Moir, L., Bochukova, E.G., Dumbell, R., Banks, G., Bains, R.S., Nolan, P.M., Scudamore, C., Simon, M., Watson, K.A., Keogh, J., et al., 2017. Disruption of the homeodomain transcription factor *orthopedia homeobox* (*Otp*) is associated with obesity and anxiety. Mol. Metabol. 6, 1419–1428.

Monaghan, A.P., Grau, E., Bock, D., Schütz, G., 1995. The mouse homolog of the orphan nuclear receptor tailless is expressed in the developing forebrain. Development 121, 839–853.

Nederbragt, A.J., Lespinet, O., van Wageningen, S., van Loon, A.E., Adoutte, A., Dictus, W.J., 2002. A lophotrochozoan twist gene is expressed in the ectomesoderm of the gastropod mollusk *Patella vulgata*. Evol. Dev. 4, 334–343.

O'Brien, J., Hayder, H., Zayed, Y., Peng, C., 2018. Overview of microRNA biogenesis, mechanisms of actions, and circulation. Front. Endocrinol. 9, 402.

Oh, H., Irvine, K.D., 2011. Cooperative regulation of growth by Yorkie and Mad through *bantam*. Dev. Cell 20, 109–122.

Oliver, G., Mailhos, A., Wehr, R., Copeland, N.G., Jenkins, N.A., Gruss, P., 1995. Six3, a murine homologue of the *sine oculis* gene, demarcates the most anterior border of the developing neural plate and is expressed during eye development. Development 121, 4055-4055.

Perkins, L.A., Holderbaum, L., Tao, R., Hu, Y., Sopko, R., MacCall, K., Yang-Zhou, D., Flockhart, I., Binari, R., Shim, H.-S., et al., 2015. The transgenic RNAi project at Harvard Medical School: resources and validation. Genetics 201, 843–852.

Ponton, F., Chapuis, M.P., Pernice, M., Sword, G.A., Simpson, S.J., 2011. Evaluation of potential reference genes for reverse transcription-qPCR studies of physiological responses in *Drosophila melanogaster*. J. Insect Physiol. 57, 840–850.

Port, F., Chen, H.-M., Lee, T., Bullock, S.M., 2014. Optimized CRISPR/Cas tools for efficient germline and somatic genome engineering in *Drosophila*. Proc. Natl. Acad. Sci. U. S. A 111, E2967–E2976.

Rubin, G.M., Spradling, A.C., 1982. Genetic transformation of *Drosophila* with transposable element vectors. Science 218, 348–353.

Rubio, M., de Horna, A., Belles, X., 2012. MicroRNAs in metamorphic and non-metamorphic transitions in hemimetabolan insect morphogenesis. BMC Genom. 13, 386.

Ruby, J.G., Stark, A., Johnston, W.K., Kellis, M., Bartel, D.P., Lai, E.C., 2007. Evolution, biogenesis, expression, and target predictions of a substantially expanded set of *Drosophila* microRNAs. Genome Res. 17, 1850–1864.
Schertel, C., Rutishauser, T., Förstemann, K., Basler, K., 2012. Functional characterization of *Drosophila* microRNAs by a novel *in vivo* library. Genetics 192, 1543–1552.
Selbach, M., Schwanhäusser, B., Thierfelder, N., Fang, Z., Khanin, R., Rajewsky, N., 2008. Widespread changes in protein synthesis induced by microRNAs. Nature 455, 58–63.
Shimoda, M., Takahashi, M., Yoshimoto, T., Kono, T., Ikai, I., Kubo, H., 2006. A homeobox gene, *prox1*, is involved in the differentiation, proliferation, and prognosis in hepatocellular carcinoma. Clin. Cancer Res. 12, 6005–6011.
Shu, X., Hildebrandt, A., Gu, J., Tannir, N.M., Matin, S.F., Karam, J.A., Wood, C.G., Wu, K., 2017. MicroRNA profiling in clear renal cell carcinoma tissues potentially links tumorigenesis and recurrence with obesity. Int. J. Mol. Sci. 18, 211.
Simeone, A., D'Apice, M.R., Nigro, V., Casanova, J., Graziani, F., Acampora, D., Avantaggiato, V., 1994. *Orthopedia*, a novel homeobox-containing gene expressed in the developing CNS of both mouse and *Drosophila*. Neuron 13, 83–101.
Sullivan, L.F., Warren, T.L., Doe, C.Q., 2019. Temporal identity establishes columnar neuron morphology, connectivity, and function in a *Drosophila* navigation circuit. Elife 8, e43482.
Takuma, N., Sheng, H.Z., Furuta, Y., Ward, J.M., Sharma, K., Hogan, B.L., Paff, S.L., Westphal, H., Kimura, S., Mahon, K.A., 1998. Formation of Rathke's pouch requires dual induction from the diencephalon. Development 125, 4835–4840.
Tessmar-Raible, K., Raible, F., Christodoulou, F., Guy, K., Rembold, M., Hausen, H., Arendt, D., 2007. Conserved sensory-neurosecretory cell types in annelid and fish forebrain: insights into hypothalamus evolution. Cell 129, 1389–1400.
Thompson, B.J., Cohen, S.M., 2006. The Hippo pathway regulates the *bantam* microRNA to control cell proliferation and apoptosis in *Drosophila*. Cell 126, 767–774.
Umesono, Y., Watanabe, K., Agata, K., 1997. A planarian *orthopedia* homolog is specifically expressed in the branch region of both the mature and regenerating brain. Dev. Growth Differ. 39, 723–727.
Umesono, Y., Watanabe, K., Agata, K., 1999. Distinct structural domains in the planarian brain defined by the expression of evolutionary conserved homeobox genes. Dev. Gene. Evol. 209, 31–99.
Vosshall, L.B., Stocker, R.F., 2007. Molecular architecture of smell and taste in *Drosophila*. Annu. Rev. Neurosci. 30, 505–530.
Wagh, D.A., Rasse, T.M., Asan, E., Hofbauer, A., Schwenkert, I., Dürrbeck, H., Buchner, S., Dabauvalle, M.-C., Schmidt, M., Qin, G., et al., 2006. Bruchpilot, a protein with homology to ELKS/CAST, is required for structural integrity and function of synaptic active zones in *Drosophila*. Neuron 49, 833–844.
Walldorf, U., Kiewe, A., Wickert, M., Ronshaugen, M., McGinnis, W., 2000. *Homeobrain*, a novel paired-like homeobox gene is expressed in the *Drosophila* brain. Mech. Dev. 96, 141–144.
Wang, W., Lufkin, T., 2000. The murine *Otp* homeobox gene plays an essential role in the specification of neuronal cell lineages in the developing hypothalamus. Dev. Biol. 227, 432–449.
Weng, M., Golden, K.L., Lee, C.-Y., 2010. dFezf/Earmuff maintains the restricted developmental potential of intermediate neural progenitors in *Drosophila*. Dev. Cell 18, 126–135.
Weng, R., Cohen, S.M., 2015. Control of *Drosophila* type I and type II central brain neuroblast proliferation by *bantam* microRNA. Development 142, 3713–3720.
Wightman, B., Ha, I., Ruvkun, G., 1993. Posttranscriptional regulation of the heterochronic gene lin-14 by lin-4 mediates temporal pattern formation in *C.elegans*. Cell 75, 855–862.
Wircer, E., Blechman, J., Borodovsky, N., Tsoory, M., Nunes, A.R., Oliveira, R.F., Levkovitz, G., 2017. Homeodomain protein Otp affects developmental neuropeptide switching in oxytocin neurons associated with the long-term effect on social behavior. Elife 6, e22170.
Wong, D.C., Lovick, J.K., Ngo, K.T., Borisuthirattana, W., Omoto, J.J., Hartenstein, V., 2013. Postembryonic lineages of the *Drosophila* brain: II. Identification of lineage projection patterns based on MARCM clones. Dev. Biol. 384, 258–289.
Wu, L., Belasco, J.G., 2008. Let me count the ways: mechanisms of gene regulation by miRNAs and siRNAs. Mol. Cell. 29, 1–7.
Yaksi, E., Wilson, R.I., 2010. Electrical coupling between olfactory glomeruli. Neuron 67, 1034–1047.
Ylla, G., Puilachs, M.D., Belles, X., 2018. Comparative transcriptomics in two extreme neopterans reveals general trends in the evolution of modern insects. iScience 4, 164–179.
Yu, H.H., Awasaki, T., Schroeder, M.D., Long, F., Yang, J.S., He, Y., Ding, P., Kao, J.C., Wu, G.Y., Peng, H., et al., 2013. Clonal development and organization of the adult *Drosophila* central brain. Curr. Biol. 23, 633–643.